DESIGN OF A LIFT REDUCTION DEVICE FOR PASSENGER CAR

GOBINATH A/L RAMAN

BACHELOR OF ENGINEERING

UNIVERSITI MALAYSIA PAHANG

2010

DESIGN OF A LIFT REDUCTION DEVICE FOR PASSENGER CAR

GOBINATH A/L RAMAN

Thesis submitted in fulfillment
of the requirements
for the award of the degree of
Bachelor of Mechanical Engineering with Automotive Engineering

Faculty of Mechanical Engineering
UNIVERSITI MALAYSIA PAHANG

DEC 2010

UNIVERSITI MALAYSIA PAHANG

FACULTY OF MECHANICAL ENGINEERING

We certify that the project entitled “Design of a Lift Reduction Device for Passenger Car” is written by Gobinath A/L Raman. We have examined the final copy of this project and in our opinion; it is fully adequate in terms of scope and quality for the award of the degree of Bachelor of Engineering. We herewith recommend that it be accepted in partial fulfillment of the requirements for the degree of Bachelor of Mechanical Engineering with Automotive Engineering.

MOHD. YUSOF TAIB
Examiner Signature

SUPERVISOR'S DECLARATION

We hereby declare that we have checked this project report and in our opinion this project is satisfactory in terms of scope and quality for the award of the degree of Bachelor of Mechanical Engineering with Automotive Engineering.

Signature :
Name of Supervisor : MUHAMMAD AMMAR BIN NIK MU`TASIM
Position : LECTURER OF MECHANICAL ENGINEERING FACULTY
Date : 6 DECEMBER 2010

STUDENT'S DECLARATION

I hereby declare that the work in this report is my own except for quotations and summaries which have been duly acknowledged. The report has not been accepted for any degree and is not concurrently submitted for award of other degree.

Signature :
Name : GOBINATH A/L RAMAN
ID Number : MH07074
Date : 6 DECEMBER 2010

This work is dedicated to my beloved ones,

My Father late Mr. Raman Muthukrishnan

My Mother Mrs. Saroja Subramaniam

My Brother Mr. Ravinthran Raman

My Sisters Ms. Sumathi Raman and Ms. Nalini Raman

AKNOWLEDGEMENTS

I would like to express my deepest appreciation and gratitude to my supervisor, Mr. Muhammad Ammar Bin Nik Mu`tasim for his guidance, patience for giving advises and supports throughout the progress of this project. Also special thanks are also given to Mr. Devarajan Ramasamy for the guidance, experience sharing and comment during PSM 1. They were not hesitant to answer all my doubts and spending their time to guide me during my experimental work.

A great appreciation is acknowledged to the Faculty of Mechanical Engineering for the funding under the final year project.

Last but not least, I would like to thank all my friends for their support and encouragement given to me, especially during the hard times.

ABSTRACT

The performance and handling of automobile are significantly affected by its aerodynamic properties. One of the main causes of aerodynamic is about lifting force. This will influence all the aspect of the vehicles such as overall performance, fuel consumption, safety and stability. The addition of rear spoiler to an aerodynamically optimized car body, leads to decrease lift coefficients. In an aerodynamic field, the main important thing to get the stability and performance is to design a vehicle with low C_L. The reduction of lift and flow separation is the key results that will be a point of discussion. Rear spoiler will reduce the flow separation at the trunk that causing the turbulent airflow. The wake region also will be reduced and this will make the lift force that produce at the rear trunk will reduce. The task was done by doing a Computational Fluid Dynamic (CFD) analysis for expected vehicle speed of 110 km/h. A lift force and drag force was obtained based on inputs from CFD analysis. This force was used to calculate the lift and drag coefficient of the model as a whole. The approach needed to justify the amount of lift that can be reduced by addition of a rear spoiler as compared to the model without the rear spoiler. This project is to get an overall comparison of the pressure distribution before and after the rear spoiler is added. Five different type of rear spoiler designed to study its effect on passenger car. The lift coefficient of the vehicle was minimized up to 0.0405 (case 4) by adding rear spoiler from 0.2036 without spoiler (case 1). This is due to the design type of spoiler in case 4 which cause greater pressure coefficient on upper wing of rear spoiler.

ABSTRAK

Ciri-ciri aerodinamik adalah sangat mempengaruhi prestasi dan kawalan sesebuah kenderaan. Salah satu kesan penyebab akan aerodinamik adalah daya tujahan. Ini akan mempengaruhi kesemua prestasi, penggunaan minyak, keselamatan, dan kestabilan sesebuah kenderaan Hasil tambahan ‘spoiler’ belakang di bahagian belakang badan kereta yang dioptimumkan secara aerodinamik menyebabkan pekali daya angkat menurun. Di dalam aspek aerodinamik, kestabilan, prestasi dan penggunaan minyak amat penting untuk menghasilkan kenderaan yang rendah C_L. Pengurangan daya angkat dan peyebaran udara adalah kunci utama di dalam perbincangan ‘spoiler’ belakang juga akan menghasilkan peyebaran pengaliran udara yang kurang di belakang kerana ini akan menghasilkan pegaliran udara yang bergelora. Kawasan olak di belakang juga akan berkurangan dan ini akan menjadikan daya angkat yang terhasil di bahagian belakang kenderaan berkurangan. Dengan nilai daya angkat yang rendah, ia akan membantu meningkatkan kestabilan kenderaan. Tugasan ini dimulakan dengan menggunakan kelajuan yang telah ditetapkan pada 110 km/j dengan menggunakan analisis Computational Fluid Dynamic (CFD). Daya angkat dapat diperolehi apabila menggunakan perisian maklumat daripada CFD analisis. Nilai daya ini akan digunakan untuk mengira pekali daya angkat keseluruhan model kereta tersebut. Nilai pengurangan daya angkat yang terhasil daripada penggunaan ‘spoiler’ belakang diperlukan untuk menbenarkan pembezaan di antara model tanpa ‘spoiler’ belakang. Projek ini akan mendapatkan perbezaan berdasarkan pegaliran angin dan tekanan sebelum dan selepas ‘spoiler’ belakang dipasangkan. Pekali daya angkat bagi kenderaan menurun dari 0.2036 kepada 0.0405 apabila ‘spoiler’ belakang dipasangkan. Hal ini berikutan reka bentuk ‘spoiler’ itu sendiri yang dapat menghasilkan pekali tekanan yang tinggi pada bahagian sayap atas ‘spoiler’ belakang.

TABLE OF CONTENTS

LIST OF TABLES

LIST OF FIGURES

LIST OF SYMBOLS

ρ	Density
V	Velocity
V_o	Wind velocity (reversed direction)
A	Area
P	Pressure
P_{atm}	Atmosphere pressure
C_D	drag coefficient
C_L	lift coefficient
C_P	pressure coefficient
F_D	Drag force
F_L	Lift force
^{o}	Degree of angle
ℓ	Length
P_{∞}	Prevailing pressure
T	Temperature
μ	Viscosity
U	Dynamic viscosity
Re	Reynolds Number
θ	Angle

LIST OF ABBREVIATIONS

CAD	Computational Aided Design
CFD	Computational Fluid Dynamic
CPU	Central Processing Unit
HPC	High Performance Computing
km/h	kilometer per hour
m/s	mile per second
mph	mile per hour
mm	millimeter
N	Newton
kPa	kilo Pascal

LIST OF APPENDICES

CHAPTER 1

INTRODUCTION

1.1 Background

The performance, handling and comfort of an automobile are significantly affected by its aerodynamics properties. Extra parts are added to the car body like rear spoiler, lower rear and front bumper and many more aerodynamics aids as to direct the air flow in different way and offer greater drag reduction and same time to enhance driving stability (Heisler, 2002).the most popular aerodynamics aid is spoiler. There are two type of spoiler, front spoiler which is also called air damn and rear spoiler. The main design purpose of a rear spoiler in vehicles is to reduce lift force and increase stability especially at rear of vehicle. Some spoilers added to car primarily for styling purpose have either little dynamic benefit or even make the aerodynamic worse. Rear spoilers, which modify the transition in shape between the rear window and trunk, act to minimize the turbulence at the rear of the vehicle (Heisler, 2002).

Many vehicles have a fairly steep downward angle going from the rear edge of the roof down to the trunk or tail of the car. At high speeds, air flowing across the roof tumbles over this edge, causing air flow separation (Heisler, 2002).The flow of air becomes turbulent and a low-pressure zone is created, increasing drag and instability. Adding a rear spoiler makes the air move a longer, gentler slope from the roof to the spoiler, which helps to delay flow separation. This decreases drag, increases fuel economy, and helps keep the rear window clean (Heisler, 2002).

1.2 Problem Statement

The main function of spoiler is to reduce lift force so the car will more stable. The concept of using rear spoiler in passenger car and how far a reduction of lift force obtained is the key interest in this study.

1.3 Objectives

The objectives of the project are as follows:

i. To compare differences between passenger car with and without lift reduction device.
ii. To analyze the flow structure on passenger car with different type of spoiler.

1.4 Scopes of Study

The scopes of the project are as follows:

i. Study the effect of spoiler on passenger car using k-ϵ turbulence model.
ii. Evaluate the stimulation using high Reynolds number of 3.75×10^6.
iii. Study the pressure coefficient on different cases of spoiler.

CHAPTER 2

LITERATURE REVIEW

2.1 Automotive Aerodynamics

Aspects of vehicle aerodynamics are no less important for the quality of an automobile such as side wind stability, wind noise, soiling of the body, the lights and the windows, cooling of the engine, the gear box and the brakes, and finally heating and ventilating of the passenger compartment all depends on the flow field around and through the vehicle (Cengel, Cimbala, 2006).

The external flow around a vehicle is shown in Figure 2.1. In still air, the undisturbed velocity V is the road speed of the car. Provided no flow separation takes place, the viscous effects in the fluid are restricted to a thin layer of a few millimeters thickness, called the boundary layer, beyond this layer the flow can be regarded as in viscid, and its pressure is imposed on the boundary layer.

Within the boundary layer the velocity decrease from the value of the in viscid external flow at the outer edge of the boundary layer to zero at the wall, where the fluid fulfill no-slip condition (Heisler, 2002). When the flow separates the boundary layer is ‘dispersed’ and the flow is entirely governed by viscous effects. Figure 2.2 shows the streamline flow of fluid around the car body.

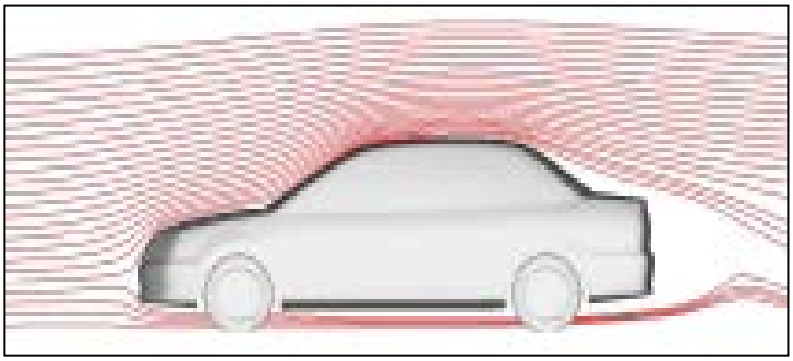

Figure 2.1: Flow around a passenger car (external flow).

Source: Koike et al. (2004)

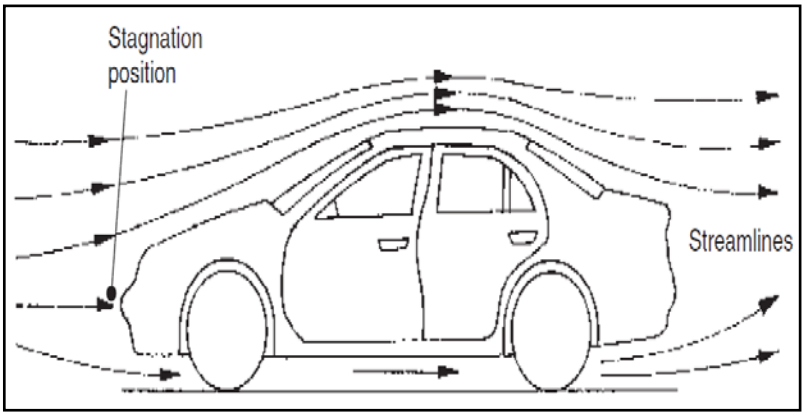

Figure 2.2: Streamline flow around the passenger car body.

Source: Heisler (2002)

2.2 Aerodynamic Force

2.2.1 Forces

A body in motion is affected by aerodynamic forces. The aerodynamic force acts externally on the body of a vehicle. The aerodynamic force is the net result of all the changing distributed pressures which airstreams exert on the car surface (Paschkewit, 2006). Aerodynamic forces interact with the vehicle causing drag, lift, down, lateral

forces, moment in roll, pitch and yaw, and noise. The aerodynamic forces produced on a vehicle arise from two sources that are form (or pressure) drag and viscous friction. Table 2.1 shows the type of forces and moment that acing on vehicle in different direction. Forces and moment are normally defined as they act on the vehicle. Thus a positive force in the longitudinal (x-axis) direction on the vehicle is forward. The force corresponding to the load on a tire acts in the upward direction and is therefore negative in magnitude (in the negative z-direction). The forces also corresponding to the shape on the vehicle part in aerodynamic shape (Cengel, Cimbala, 2006). Figure 2.3 below shows arbitrary force and origin of the forces that acting on the vehicle.

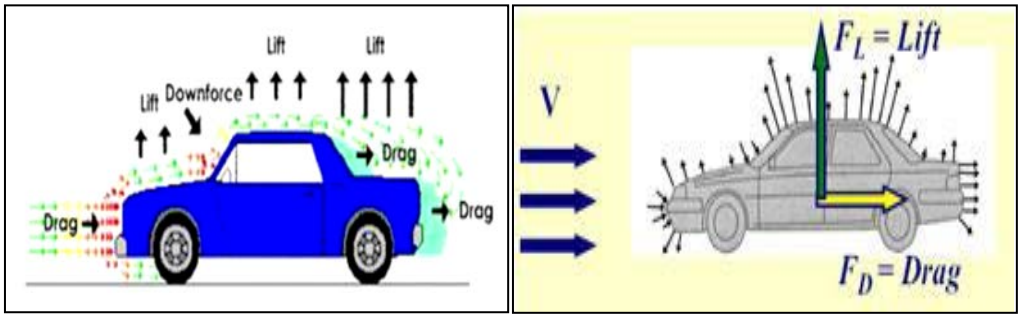

Figure 2.3: Arbitrary forces and origin of the forces acting on the vehicle.

Source: Cengel, Cimbala (2006)

Table 2.1: Forces acting on moving vehicle.

Direction	Force	Moment
Longitudinal (*x*-axis, *+ve* rearward)	Drag	Rolling moment
Lateral (*y*-axis, *+ve* to the right)	Side force	Pitching moment
Vertical (*z*-axis, *+ve* upward)	Lift	Yawing moment

Source: Hirsch (2007)

The focus in cars is on the aerodynamic forces of down force and drag. The relationship between drag and down force is especially important. Aerodynamic improvements in wings are directed at generating down force on the car with a minimum of drag. Down force is necessary for maintaining speed through the corners (Paschkewit, 2006).

2.2.2 Lift Force

The airflow around vehicle usually cause lift force. The components of the pressure and wall shear stress in the direction normal to the flow (perpendicular) tend to move the body in that direction, and their sum is called lift. To some degree, body panel shape and to a larger extent, air that passes through the opening of the grille and under the front end sheet metal. At speed, this massive air stream builds up tremendous pressure under the hood where it is forced to exit rearward, below the chassis, resulting in body lift (Cengel, Cimbala, 2006).

Lift can effectively countered by limiting the amount of air flowing under the front sheet metal with the use of "dams" and by down-sizing the opening in the grille. Furthermore, we can relieve pressure under the hood by incorporating exhaust vents in the fenders such as the ones used on the Trans-Am Firebirds and Corvettes. Lift force can be determined from equation 2.1(Cengel, Cimbala, 2006). Any remaining lift may be countered by applying down force using additional aerodynamic spoiler devices at the front and rear of the vehicle. The lift of the vehicle is characterized by the lift coefficient (C_L) and can be calculated by using equation 2.2 (Cengel, Cimbala, 2006). Figure 2.4 shows lift force acted in airfoil.

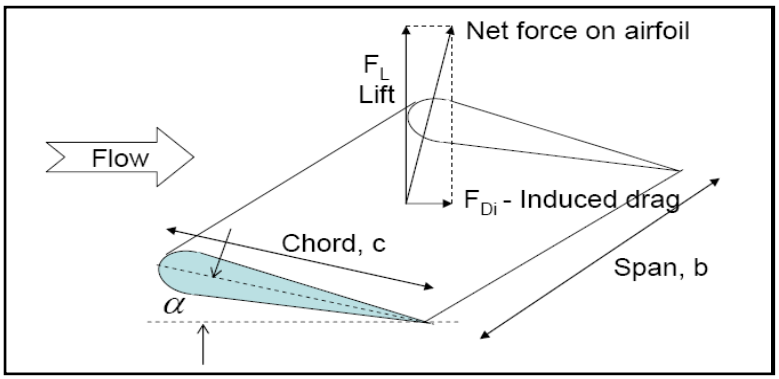

Figure 2.4: Lift force acted in airfoil

Source: Cengel, Cimbala (2006)

Lift Force:

$$F_L = \frac{1}{2} C_L \rho v^2 A \quad (2.1)$$

Lift Coefficient:

$$C_L = \frac{2F_L}{\rho v^2 A} \quad (2.2)$$

Where:

F_L = lift force [N]
C_L = lift coefficient
ρ = density of the air [kg/m3]
A = area of the body [m2]
V = velocity of the body [m/s]

2.2.3 Drag Force

Drag Force is the force a flowing fluid exerts on a body in the flow direction. Drag force consists of skin drag and pressure drag. Equation 2.3 (Cengel, Cimbala, 2006) shows relation between friction drag and pressure drag. Frontal pressure is caused by the air attempting to flow around the front of the car. As millions of air molecules approach the front part of the car, they begin to compress, and in doing so raise the air pressure in front of the car. Rear vacuum or wake is caused by the "hole" left in the air as the car passes through it. This empty area is a result of the air molecules not being able to fill the hole as quickly as the car can make it (Cengel, Cimbala, 2006). The air molecules attempt to fill in to this area, but the car is always one step ahead.

In every moving vehicle, the drag will produce in every surface of the vehicle. The drag is due in part to friction of the air on the surface of the vehicle, and in part to the way the friction alters the main flow down the back side of the vehicle. Drag is the largest and most important aerodynamic force encountered by passenger cars at normal

highway speeds. Drag force is summation of friction drag force and pressure drag force and the equation 2.3 is the relation between drag force, friction drag, and pressure drag where $F_{D,\ fric\ is}$ friction drag and $F_{D,\ press}$ is pressure drag (Cengel, Cimbala, 2006). The overall drag on a vehicle derives from contributions of many sources. For the vehicle, the drag produced from the body (for body, after body, under body and skin friction). The major contributor is the after body because of the drag produced by the separation zone at the rear. It is in area that the maximum potential for drag reduction is possible (Cengel, Cimbala, 2006).

$$F_D = F_{D,fric} + F_{D,press}\ , \tag{2.3}$$

Drag coefficient is the dimensionless ratio of the drag force to the dynamic pressure force of the free stream. The aerodynamic drag is the focus of public interest in vehicle aerodynamics. It is and even more so it's non-dimensional number of C_D, the drag coefficient has almost become a synonym for the entire discipline.

Performance, fuel economy, emissions, and top speed are important attributes of a vehicle because they represent decisive sales arguments, and they all are influenced by drag. Drag coefficient (C_D) is a commonly published rating of a car's aerodynamic smoothness, related to the shape of the car. Multiplying C_D by the car's frontal area gives an index of total drag. The result is called drag area, and is listed below for several cars. The width and height of curvy cars lead to gross overestimation of frontal area. The aerodynamic drag coefficient equation is (2.5) (Cengel, Cimbala, 2006):

Drag Force:

$$F_D = \frac{1}{2} C_D \rho v^2 A \tag{2.4}$$

Drag Coefficient:

$$C_D = \frac{2F_D}{\rho v^2 A} \quad (2.5)$$

Where:

F_D = drag force [N]

C_D = drag coefficient

ρ = density of the air [kg/m3]

A = area of the body [m2]

V = velocity of the body [m/s]

A low drag coefficient implies that the streamline shape of the vehicle's body is such as to enable it to move easily through the surrounding viscous air with the minimum of resistance, conversely a high drag coefficient is caused by poor streamlining of the body profile so that there is a high air resistance when the vehicle is in motion (Heisler, 2002). Typical drag coefficient for various classes of vehicle can be seen in Table 2.2

Table 2.2: Typical drag coefficient for various classes of vehicle.

Vehicle type	**Drag coefficient C_D**
Saloon car	0.22-0.40
Sports car	0.28-0.40
Light van	0.35-0.50
Buses and coaches	0.40-0.80
Articulated trucks	0.55-0.80
Ridged truck and draw bar trailer	0.70-0.90

Source: Heisler (2002)

The drag coefficient varies over a board range with different shapes. Figure 2.5 below shows the coefficients for a number of shapes. In each case it is presumed that the air approaching the body has no lateral component. The simple aerofoil has a drag

coefficient of 0.007. This coefficient means that the drag force is 0.007 times as large as the dynamic pressure acting over the area of the plate.

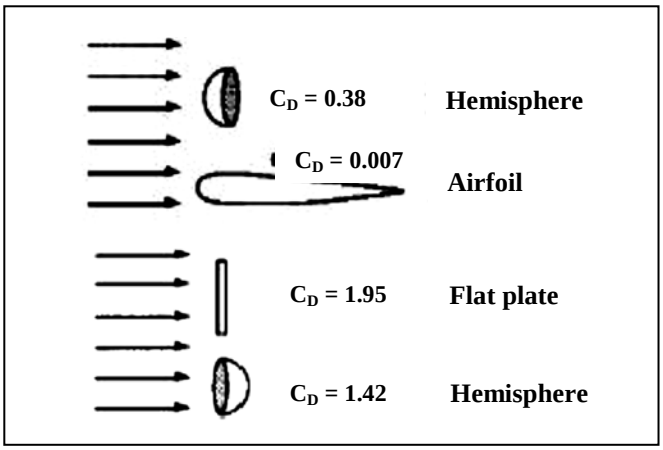

Figure 2.5: Drag coefficients of various shapes.

Source: Cengel, Cimbala (2006)

2.3 Aerodynamic Pressure

The gross flow over the body of a vehicle is governed by the relationship between velocity and pressure expressed in Bernoulli's Equation. Bernoulli's Equation assumes incompressible flow which is reasonable for automotive aerodynamics (Cengel, Cimbala, 2006).

$$P_{static} + P_{dynamic} = P_{total} \tag{2.6}$$

$$Ps + \frac{1}{2} \rho V^2 = Pt \tag{2.7}$$

Where:

ρ = density of air [kg/m3]
V = velocity of air (relative to the car) [m/s]

In equation above, the sum of the forces brings in the pressure affect acting on the incremental area of the body of fluid. The static plus the dynamic pressure of the air will be constant (Pt) as it approaches the vehicle. At the distance from the vehicle the static pressure is simply the ambient, or barometric, pressure (P_{atm}). The dynamic pressure is produced by the relative velocity, which is constant for all streamlines approaching the vehicle. As the flow approaches the vehicle, the streamlines split, some going above the vehicle and others below. By inference, one streamline must go straight to the body and stagnate (impinging on the bumper of the vehicle). At that point the relative velocity has gone to the zero. This will make the static pressure observed at that point on the vehicle. Figure 2.6 and Figure 2.7 below showing flow over a cylinder that it affects is most same to the vehicle (Cengel, Cimbala, 2006).

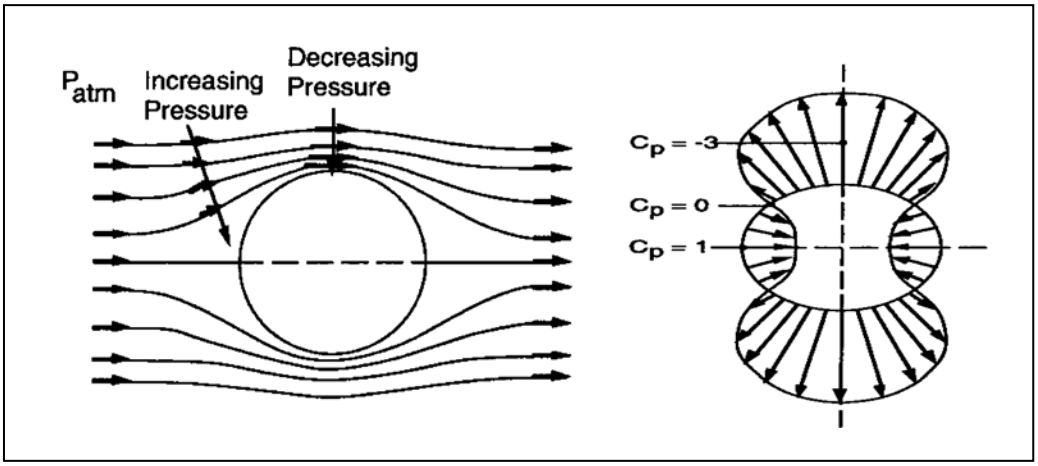

Figure 2.6: Pressure and velocity gradients in the air flow over the body.

Source: Cengel, Cimbala (2006)

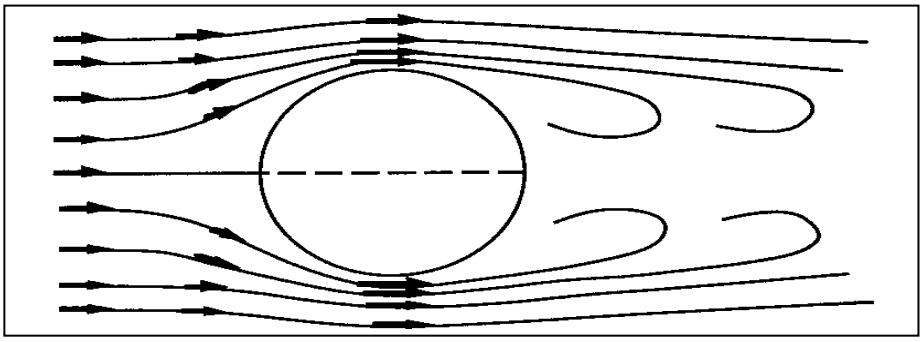

Figure 2.7: Vortex shedding in flow over a cylindrical body.

Source: Cengel, Cimbala (2006)

The static pressure will distribute along the body of a car. The pressures are indicated as being negative or positive with to the ambient pressure at some distance from the vehicle. A negative pressure is developed at the front edge of the hood as the flow rising over the front of the vehicle attempts to turn and follow horizontally along the hood (Cengel, Cimbala, 2006). Near the base of the windshield and cowl, the flow must be turned upward, thus the high pressure is experienced. Over the roof line the pressure goes negative as the air flow tries to follow the roof contour.

2.4 Air Flow around the Vehicle

Under calm conditions and no traffic, vehicles travel through still air, hence the relative air flow they experience has no turbulence, is unsteadily relative to the vehicle and has the same magnitude as the vehicle speed relative to the road. If an atmospheric wind or air flow is present, generally a yaw angle is created because the flow is not aligned with the centerline of the vehicle and thus the air speed of a vehicle experiences is not the same as the road speed (Jeong et al., 2007)

The flow processes to which a moving vehicle is subjected fall into two categories which are flow of air around the vehicle and flow of air through the vehicle's body. The two categories of these flow fields are closely related. For example, the flow of air through the engine compartment depends on the flow field around the vehicle. Both flow fields must be considered together. On the other hand, the flow processes within the engine and transmission are not directly connected with these two categories

of flow. They are not called aerodynamics, and are not treated here (Ferlauto, Marsilio, 2006). Flow separations may appear in different locations on vehicles with more angular geometries, and fairing dominated flows can exist on a variety of road vehicles. The main aspect of this flow field is the formation of two concentrated side edge vortices which dominate the nearby flow field. Those two vortices induce a large velocity on the plate creating strong suction forces which considerably increase the lift of the flat-plate wing. Typical pattern of flow-separation frequently found on three-box-type sedans. In this case a separated bubble, with locally recirculation flow, is observed in the front, at the break point between the bonnet and the windshield. The large angle created between the rear windshield and trunk area results in a second, similar flow-recirculation area (Heisler, 2002; Regert, Lajos, 2006).

2.4.1 External Flow

The external flow around a passenger car is shown in Figure. 2.2. In still air, the undisturbed velocity *V* is the road speed of the car. Provided no flow separation takes place, the viscous effects in the fluid are restricted to a thin layer of a few millimeters thickness, called the boundary layer. Beyond this layer the flow can be regarded as inviscid, and its pressure is imposed on the boundary layer. Within the boundary layer the velocity decreases from the value of the inviscid external flow at the outer edge of the boundary layer to zero at the wall, where the fluid fulfills a no-slip condition. When the flow separates the boundary layer is "dispersed" and the flow is entirely governed by viscous effects (Najmudin, 2001).

Such regions are quite significant as compared to the characteristic length of the vehicle. At some distance from the vehicle there exists no velocity difference between the free stream and the ground. Therefore, in vehicle-fixed coordinates, the ground plane is a stream surface with constant velocity *V*, and at this surface no boundary layer is present. This fact is very important for the simulation of flows around ground vehicles in wind tunnels. Figure 2.8 illustrate the boundary layer around aerfoil.

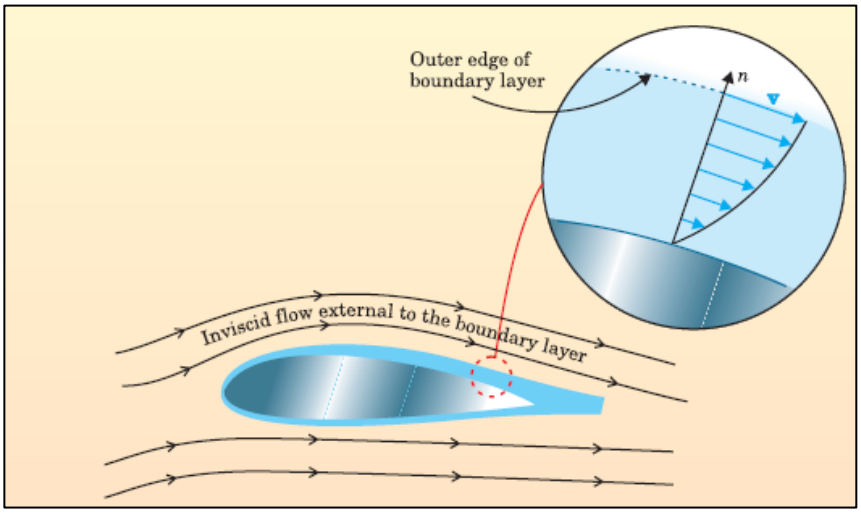

Figure 2.8: Boundary layer.

Source: Najmudin (2007)

Provided no flow separation takes place, the viscous effects in the fluid are restricted to a thin layer of a few millimeters thickness, called the boundary layer. Beyond this layer the flow can be regarded as in viscid, and its pressure is imposed on the boundary layer. Within the boundary layer the velocity decreases from the value of the in viscid external flow at the outer edge of the boundary layer to zero at the wall, where the fluid fulfills a no slip condition. When the flow separates, the boundary layer is "dispersed" and the flow is entirely governed by viscous effects. The character of the viscous flow around a body depends only on the body shape and the Reynolds number. For different Reynolds numbers entirely different flows may occur for one and the same body geometry. Thus the Reynolds number is the dimensionless parameter which characterizes a viscous flow (Heisler, 2002).

2.5 Dynamic Fluid Properties

2.5.1 Air Density Properties Related to Vehicle

The air density is variable depending on temperature, pressure, and humidity conditions. The air density must be expressed as mass density, obtained by dividing by the acceleration of gravity. Density at other conditions can be estimated for the prevailing pressure, *P* and temperature, T conditions by the equation below (Cengel, Cimbala, 2006).

The highest speeds achieved by land-vehicles during record attempts are on the order of the speed of sound which is for air, = 330 m/s = 1225 km/h = "65.6 mph. In the flow field of a body exposed to such a free stream the compressibility of the air is very important. On the other hand, most vehicles including racing cars are operated at speeds which are lower than one-third of the speed of sound. For this speed range the variations of pressure and temperature in the flow field are small as compared to free-stream values, and therefore the corresponding changes of density can be neglected. Thus the fluid can be regarded as incompressible (Cengel, Cimbala, 2006).

2.5.2 Air Viscosity Properties Related to Vehicle

The air will have its own viscosity when the car is moving through the air surrounding. Viscosity is caused by the molecular friction between the fluid particles. It relates momentum flux to velocity gradient, or applied stress to resulting strain rate. According to Newton's law for the flow parallel to a wall, the shear stress, τ is proportional to the velocity gradient *du/dy*. The constant factor *U* is a property of the fluid called dynamic viscosity. In general its value depends on the temperature (Reget, Lajos, 2006). Often the quotient $\nu = \mu/\rho$ is used, which is called kinematics viscosity and which depends on pressure and temperature (Regert, Lajos, 2006). For incompressible fluids, only temperature dependence exists for ν and μ. The viscosity of a real fluid is the physical reason for the occurrence of a friction drag in the presence of a velocity gradient at a wall. It is same case in surface contact of the vehicle as when the vehicle is moving in any velocity.

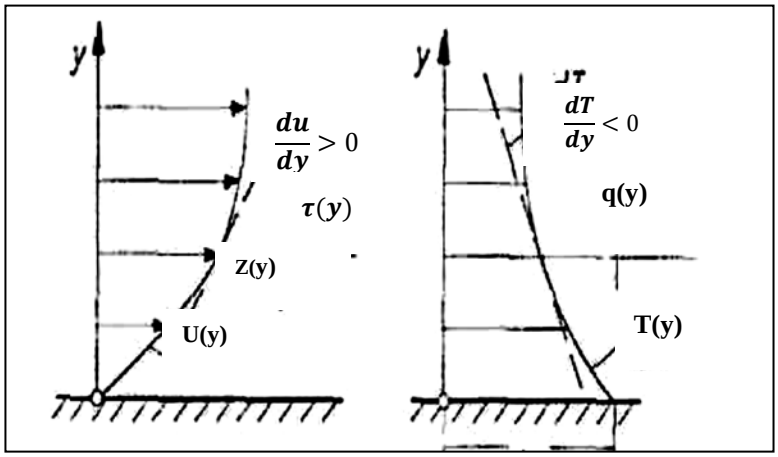

Figure 2.9: Distribution of velocity and temperature in the vicinity of a wall.

Source: Regert, Lajos (2006)

2.6 Friction Drag

The pressure in the separation region is below that imposed on the front of the vehicle, and the difference in these overall pressure forces is responsible for 'from drag'. The drag forces arising from the action of viscous friction in the boundary layer on the surface of the car is the friction drag. In the boundary layer, the velocity is reduced because of friction (Cengel, Cimbala, 2006). In a viscous fluid a velocity gradient is present at the wall. Due to molecular friction a shear stress acts everywhere on the surface of the body as indicated in Figure 2.10 below .The integration of the corresponding force components in the free-stream direction leads to the so-called friction drag. In the absence of flow separation, this is the main contribution to the total drag of a body in two-dimensional viscous flow.

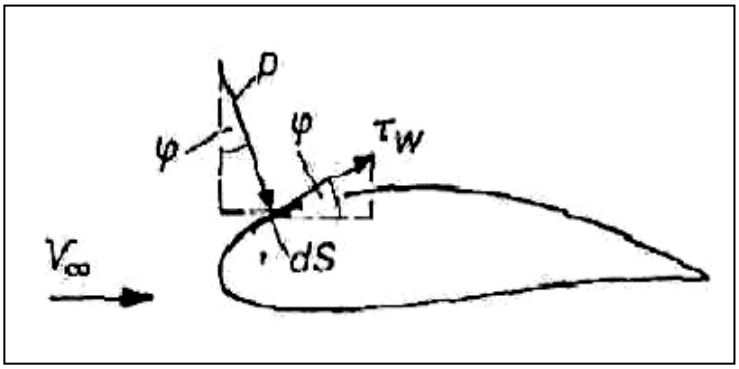

Figure 2.10: Determination of the drag of a body (two-dimensional flow).

Source: Heisler (2002)

2.7 Reynolds Number

The general factors of drag, aerodynamic friction, are density and viscosity of the fluid, air being considered a fluid. The definition of Reynolds Number is shown at above (Heisler, 2002). The Reynolds Number for a body that is large in size and slow in velocity could produce an equivalent Reynolds Number of a very small object that travels with a high velocity. This seems like it isn't possible logically until we evaluate the definition Reynolds Number and see that it is. At high Reynolds numbers, typical of full-sized car, it is desirable to have a laminar boundary layer. This results in a lower skin friction due to the characteristic velocity profile of laminar flow. At lower Reynolds numbers, such as those seen with model car, it is relatively easy to maintain laminar flow. This gives low skin-friction, which is desirable. However, the same velocity profile which gives the laminar boundary layer its low skin friction also causes it to be badly affected by adverse pressure gradients. As the pressure begins to recover over the rear part of the rear hood, a laminar boundary layer will tend to separate from the surface. Such separation causes a large increase in the pressure drag, since it greatly increases the effective size of the rear hood section (Heisler, 2002). Equation 2.8 is equation for Reynolds number

$$\text{Reynolds number}, Re = \frac{\rho l v}{\mu} \tag{2.8}$$

Where:

ρ = density of the fluid

l = characteristic of length

v = velocity of the body in the fluid

μ= viscosity of the fluid

2.8 Computational Fluid Dynamics

Computational Fluid Dynamics, known today as CFD, is defined as the set of methodologies that enable the computer to provide us with a numerical simulation of fluid flows. The word 'simulation' used to indicate that the computer to solve numerically the laws that govern the movement of fluids, in or around a material system, where its geometry is also modeled on the computer. Hence, the whole system is transformed into a 'virtual' environment or virtual product. This can be opposed to an experimental investigation, characterized by a material model or prototype of the system, such as an aircraft or car model in a wind tunnel, or when measuring the flow properties in a prototype of an engine (Najmudin, 2007).

This terminology is also referring to the fact that we can visualize the whole system and its behavior, through computer visualization tools, with amazing levels of realism, as you certainly have experienced through the powerful computer games and/or movie animations, which provide a fascinating level of high-fidelity rendering. Hence the complete system, such as a car, an airplane, a block of buildings, etc. can be 'seen' on a computer, before any part is ever constructed (Najmudin, 2007).

Performing CFD analysis on a large data set such as one that represents a moving car or a fighter jet requires considerable CPU resources that can take a long time to process. To address this issue, some independent software vendors (ISVs) offering CFD applications have made their applications parallel and cluster-aware. By leveraging the parallel-processing capabilities of high performance computing (HPC)

clusters, CFD applications can enable large data sets that require heavy-duty CPU resources to run faster than they could run on a single server (Najmudin, 2007).

An HPC cluster can be created using standard, off-the shelf components that work together as a supercomputer. HPC cluster designers have the flexibility to choose from multiple options for the base computing platform, subsystems, and interconnect. Platforms for HPC clusters are available in a variety of configurations, using different processor types and speeds, cache sizes, disk I/O, and memory subsystems. To create an optimal HPC cluster for use with a specific CFD application, the designer must understand the performance characteristics of the application itself and the effects of the various subsystem components on the application. This knowledge allows the designer to allocate resources to the proper components and to budget adequate financial resources to build an optimal system (Najmudin, 2007).

2.9 k–e Turbulence Model

To account for the turbulence effect on the flow field, Reynolds time averaging technique was employed on the Navier-Stokes equation to yield the Reynolds Averaged Navier-Stokes (RANS) equation which can be mathematically expressed as equation 2.9

$$\frac{\partial \bar{u}_i}{\partial t} + \bar{u}_j \frac{\partial \bar{u}_i}{\partial x_j} = -\frac{1}{\rho}\frac{\partial \bar{p}}{\partial x_i} + \frac{\partial}{\partial x_j}\left(v\frac{\partial \bar{u}_i}{\partial \bar{u}_j} - \bar{\tau}_{ij}\right) \qquad (2.9)$$

Where:

$$i = 1, 2, 3,;$$
$$j = 1, 2, 3,;$$

The bar on top of the variables implies that the variables are the time-averaged quantities. In Eq. (2.9), sij is the shear-stress tensor. Eq. (2.9) is impossible to resolve due to the appearance of the Reynolds stress. To bring closure to the above equation, the Reynolds stress term is modeled through the means of k–e turbulence modeling technique (Tsai et al., 2007).

The k–e turbulence model is usually applied to simulate air flow fields in mechanical ventilation system and in other modern engineering applications. In the early stage of research, turbulence model was only applied for incompressible high Reynolds number flows but it was later experimentally proven that air flows next to solid walls were associated with low Reynolds numbers. Therefore, the development and testing of low Reynolds number turbulence models have been a topic for extensive research (Tsai et al., 2007). A remedy to this approach is the introduction of a wall function into the modeling so that the airflow within the entire computational domain can be calculated using equation 2.10 and equation 2.11 at the same time even if the Reynolds number near the walls is low while that far away from the wall is high.

$$\frac{\partial(\rho k)}{\partial t} + u_i \frac{\partial(\rho k)}{\partial x_i} = \frac{\partial}{\partial x_i}\left(\frac{\mu_t}{\sigma_k}\frac{\partial k}{\partial x_i}\right) + G - \rho\varepsilon \qquad (2.10)$$

Where:

i = 1, 2, 3,

$$\frac{\partial(\rho\varepsilon)}{\partial t} + u_i \frac{\partial(\rho\varepsilon)}{\partial x_i} = \frac{\partial}{\partial x_i}\left(\frac{\mu_t}{\sigma_\varepsilon}\frac{\partial \varepsilon}{\partial x_i}\right) + C_{1\varepsilon}\frac{\varepsilon}{k}G - C_{2\varepsilon}^{*}\rho\frac{\varepsilon^2}{k} \qquad (2.11)$$

Where:

i = 1, 2, 3,

The turbulence model used in this work is the RNG k–e turbulence model because of its good prediction of complex flows (Tsai et al., 2007). The complete formulation of the RNG k–e turbulence model is given in Einstein summation convention as follows

$$G = 2\mu_t S_{ij} S_{ij} \qquad (2.12)$$

$$C_{2\varepsilon}^{*} = C_{2\varepsilon} + C_{2\varepsilon}' \qquad (2.13)$$

$$C'_{2\varepsilon} = \frac{C_\mu \rho \eta^3 (1 - {\eta}/{\eta_0}}{1 + \beta \eta^3} \quad (2.14)$$

$$\mu_t = \rho C_\mu \frac{k^2}{\varepsilon} \quad (2.15)$$

$$\eta = S\frac{k}{\varepsilon} \quad (2.16)$$

$$S = \sqrt{2S_{ij}S_{ij}} \quad (2.17)$$

Where S_{ij} the shearing-rate tensor, and g_i is the body force in the x_i direction (Tsai et al., 2007)

CHAPTER 3

METHODOLOGY

3.1 Introduction

The methodology for this project must be set effectively in order to achieve the objective of the project. Methodology will be the guideline from the beginning until the project is complete. This chapter also helps from not deviate from our topic and project scope. All method or procedure that involved in this project is in included in this chapter. The title “Design of a Lift Reduction Device for Passenger Car” was given by supervisor on the beginning of the semester. The literature study that related to this topic has been carried out in Chapter 2.

This project is basically about designing and analyzing lift reduction device that is capable of reducing lift force on a passenger car. Hence it involves analyzing the effect of rear spoiler on passenger car in terms of pressure, velocity, and lift by using Computational Fluid Dynamic (CFD). Figure 3.1 shows the methodology flow chart with the work description for PSM

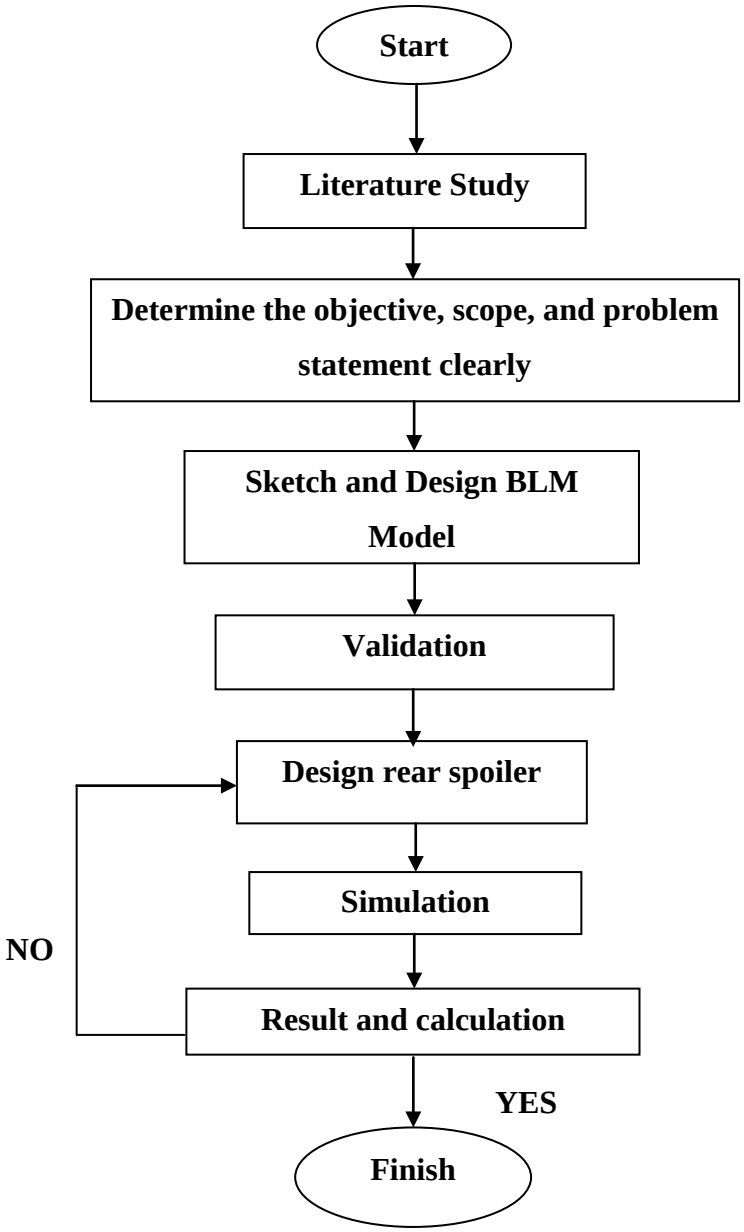

Figure 3.1: Methodology flow chart for PSM.

3.2 Problem Solving

The main problem solving tools used in this project is Computational Fluid Dynamics (CFD) which is used to stimulate flow velocity, υ and pressure, p distribution around the vehicle body with and without rear spoiler. The steps involved in problem solving follows the methodology flow chart to ensure that the work progress goes smoothly.

3.2.1 3-D Car Modeling

The 3D car model used for this project is Proton Saga BLM 2008. The dimension of the model is approximately same to real car dimension from Proton Manual Book. Some part of the actual car are not included in 3D modeling such as fender and side mirror and some part not same as actual car such as underbody of car. The Figure 3.2 to Figure 3.5 shows 3D model of Saga BLM in different views.

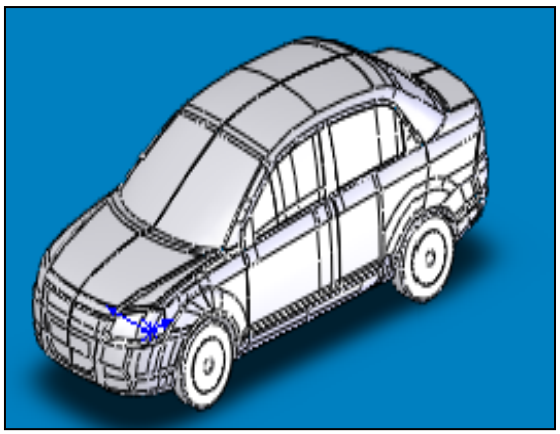

Figure 3.2: Isometric View of Saga BLM.

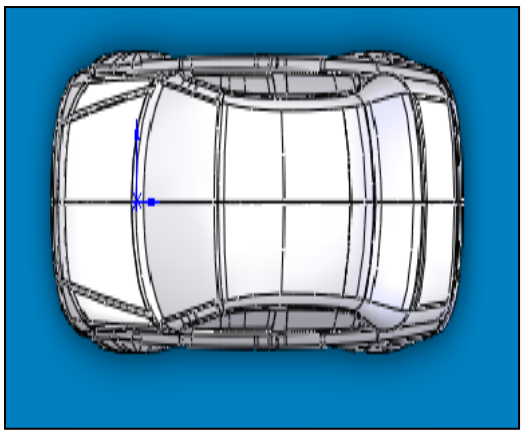

Figure 3.3: Top View of Saga BLM.

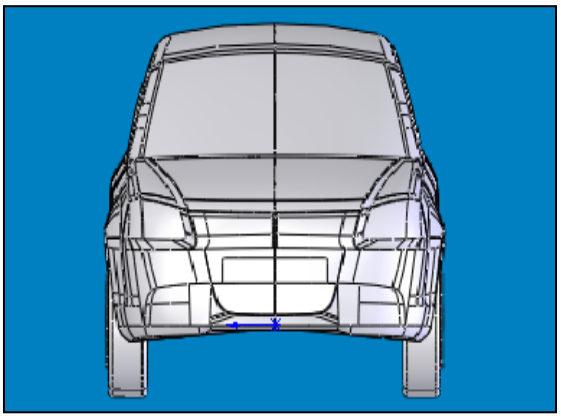

Figure 3.4: Frontal View of Saga BLM.

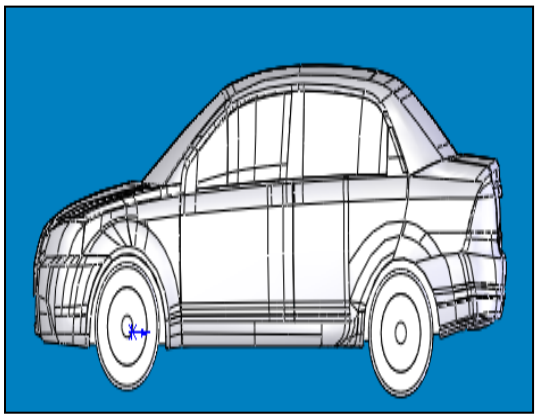

Figure 3.5: Side View of Saga BLM.

3.2.2 Validation

The validation has been done by Tsai et al. (2007) to compare the result between CFD analysis and experimental. For validation, a 2D cylinder case was studied with a record point inserted in the computational domain as shown in Figure 3.6 to monitor the pressure variation. The point is 1.3 m away from the center of the cylinder and h =45° above the horizontal axis. The radius of the 2D cylinder is 10 mm. The left, top, and bottom boundaries were assumed inlets with a prescribed horizontal velocity of V= 40 m/s that corresponded to Re = 2.75 10.The right boundary was modeled as an outlet whose pressure was fixed at 1 atm. The result of validation shown in Figure 3.7 where the pressure coefficient obtained by using CFD simulation is almost same with the result for experimental.

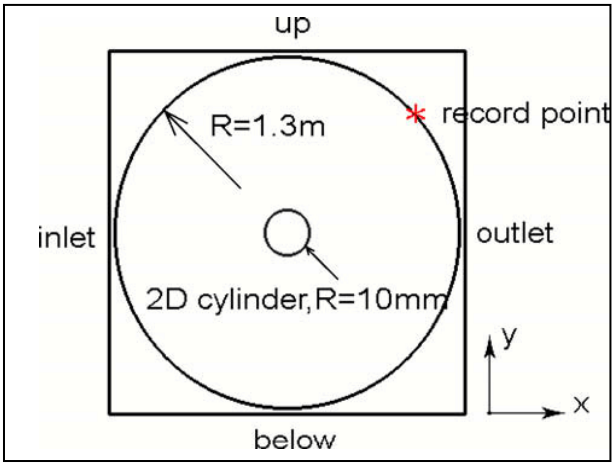

Figure 3.6: The 2D cylinder model for validation.

Source: Tsai et al. (2007)

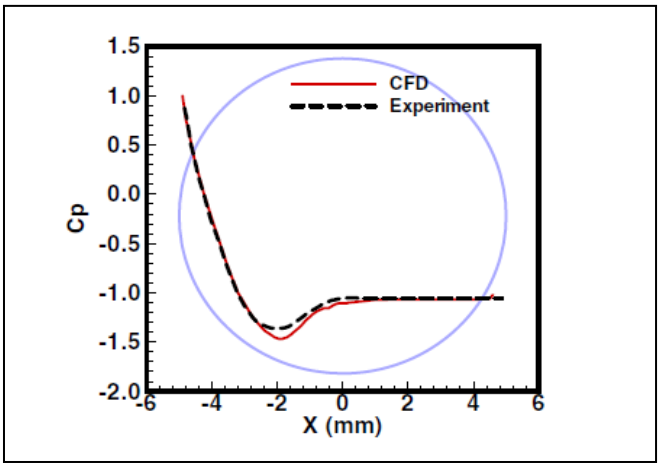

Figure 3.7: Comparison between CFD and experimental.

Source: Tsai et al. (2007)

The Figure 3.8 shows the comparison between Tsai et al. model with Saga BLM. The result is for 1st case (without spoiler) of both models. Both models give highest pressure coefficient at point 1 which is located at bumper of car model. This is due to the stagnation point where the pressure separation regions cause higher total pressure. The pressure coefficient decrease at 0.5 m because of the streamline body shape at hood caused pressure to drop. The pressure again increases at windscreen for both cases because of pressure drag. The pressure coefficient is negative at roof of the car for both

cases. These pressure coefficient increases at trunk area (2m-4m) due to the increases in air velocity. The increases in air velocity cause increase in pressure. There are slight differences between the trends of the graph of both models because the type of model used for the analysis where C.H Tsai used Honda S2000 as the model for the analysis while in this study Saga BLM model is used.

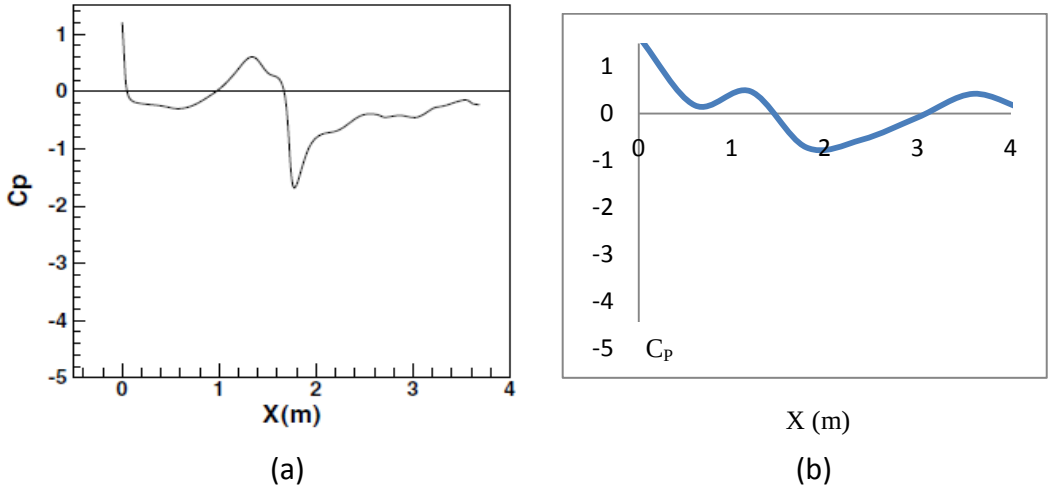

Figure 3.8: Comparison between Tsai et al. model (a) with Saga BLM (b).

3.2.3 Five Type of Spoiler Design

To study the effect of the installation spoiler on the aerodynamics aspect of the passenger car, six cases were considered. As shown in Figure 3.9(a), case 1 is base model which corresponds to a car without spoiler. Figure 3.9(b) to Figure 3.9(f) shows five type of spoiler with different cross-section profile that was considered in this study. Figure 3.9(b) is single-wing type spoiler while Figure 3.9(c) is single-wing with side cover type spoiler. Figure 3.9(d) is double-wing (upper wing behind lower wing) type spoiler model. Figure 3.9(e) is double-wing (upper wing and lower wing aligned) type spoiler and Figure 3.9(f) is double-wing (upper wing in front lower wing) type spoiler.

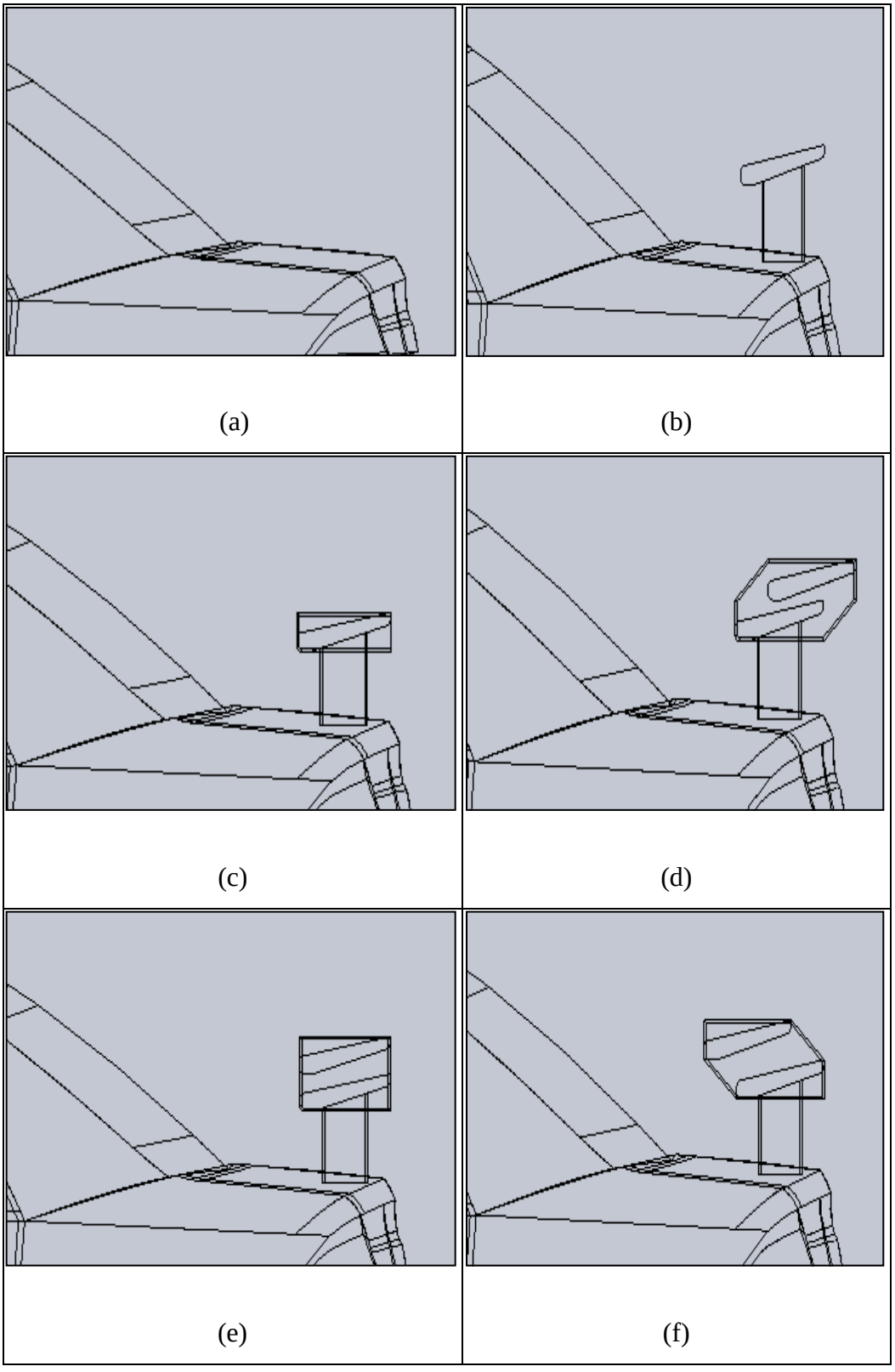

Figure 3.9: Configuration of spoiler on the Saga BLM trunk.

3.2.4 CFD Simulation

The car model transferred into Computational Fluid Dynamics (CFD) Simulation to analyze the flow velocity and the pressure distribution around the car model body. Through this simulation also, the drag coefficient and lift coefficient can be determined by setting the goals in tree view. The simulation will be done for car model without spoiler and also car model with spoiler to obtain the differences in term velocity, pressure, and lift coefficient for both car model. Some parameters of boundary condition such as velocity, temperature, pressure, and flow type must be set first. Figure 3.10 shows the boundary condition for car model without spoiler. Same boundary condition fixed for simulate car model with spoiler. The size of boundary condition is 15 m between minimum x-axis and maximum x-axis, 10 m between minimum y-axis and maximum y-axis, and 7 m between minimum z-axis and maximum z-axis.

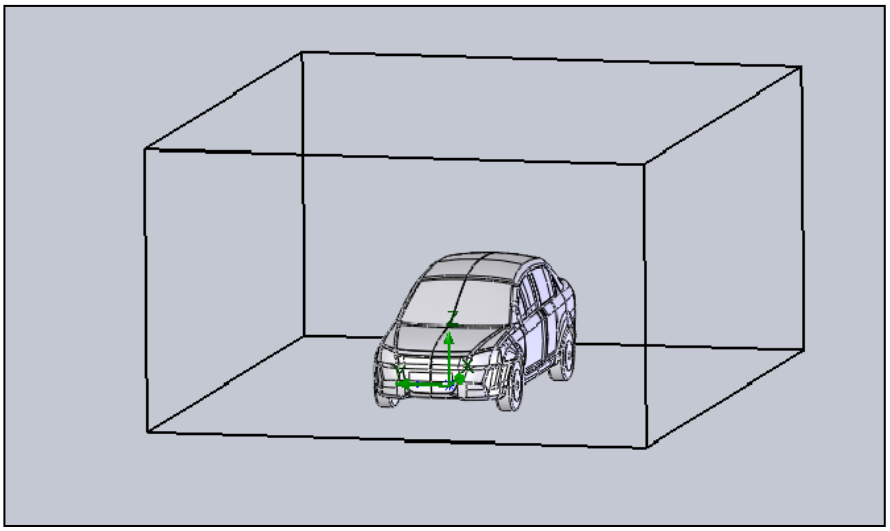

Figure 3.10: Boundary condition size for car model without spoiler.

The type of flow used is external flow because only the velocity flow and pressure distribution around the car model to be observed. The air flow value is 110 km/h which is maximum allowable speed limit of Malaysian highways. Figure 3.11 shows the parameters that fixed before run the simulation. Pressure is standard atmosphere pressure 101.325 kPa while temperature used is 293.2 K. Velocity of fluid flow (air) is 30.56 m/s which is correspond to 110 km/h in x-axis direction.

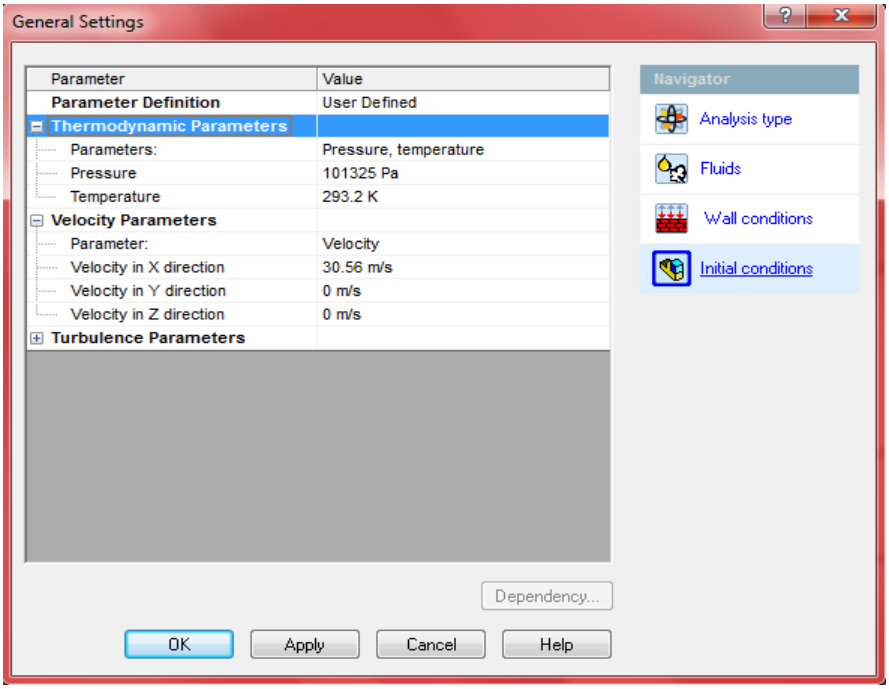

Figure 3.11: General setting for CosmoFlow Work's simulation.

CHAPTER 4

RESULT AND DISCUSSION

4.1 Introduction

The main objective of this project is about to study the effect of rear spoiler on pressure distribution. The effect will be simulated before and after the adding of rear spoiler using the CFD simulation. In automotive design studies, the aerodynamic devices such as rear spoiler are the important part in designing a vehicle. This aerodynamic device will influence of the stability, performance, fuel consumption and others on the vehicle.

4.2 Result and Calculation

4.2.1 Total Pressure and Pressure Coefficient

Pressure distribution over the top of car body analyzed by setting point global at certain location of car body so the pressure value of that point obtained. The black color point in the Figure 4.1 shows the location where the pressure value taken on car model for case 1. Table 4.1 is the total pressure distribution value and pressure coefficient according to sequence of point for all six cases the considered. Distance, x in meter is the location of point along x-axis.

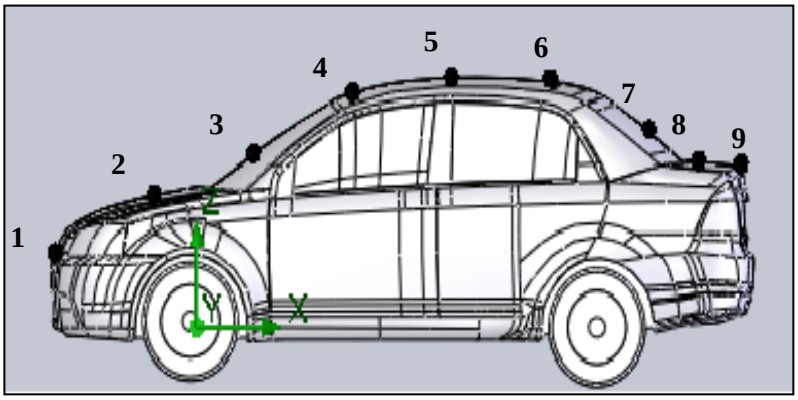

Figure 4.1: Pressure point location for case 1.

The data obtained from the simulation result used to calculate pressure coefficient. Sample of the calculation are as follow:

$$\text{Pressure coefficient, } C_p = \frac{P - P\infty}{\frac{1}{2}\rho\infty V\infty^2} \qquad (4.1)$$

Where:

Total pressure, P = 101.566 kPa

Upstream pressure, P_∞ = 101.376 kPa

Upstream density, ρ_∞ = 1.200 kg/ms

Upstream velocity, V_∞ = 30.56 m/s

Solution:

$$Cp = \frac{(1022945 - 101376)\text{Pa}}{\frac{1}{2} \times \left(1.200\,\frac{\text{kg}}{\text{m}^2}\right) \times (30.56\,\frac{\text{m}}{\text{s}})^2}$$

= 1.6392

Table 4.1 is the result of total pressure and pressure coefficient obtained for case 1.Distance x in meter is the location of point along x-axis.

Table 4.1: Total pressure and pressure coefficient of car body for case 1.

No. of Points	X(m)	Total Pressure [kPa]	Pressure coefficient,C_D
1	0	102.2945	1.6392
2	0.6	101.4769	0.1801
3	1.2	101.6435	0.4774
4	1.8	100.9732	-0.7188
5	2.4	101.0644	-0.5542
6	3.0	101.3321	-0.0783
7	3.6	101.6137	0.4242
8	4.2	101.4085	0.0581
9	4.5	101.4557	0.1422

Figure 4.2 show pressure coefficient distributions on top body of Saga BLM for case 1 which is without addition of rear spoiler. Point 1 which located at front bumper gives highest pressure coefficient value of 1.6392. This is due to the stagnation point where the pressure is in separation region cause the higher total pressure. The pressure is dominant for front bumper because its blunt body shape. The pressure coefficient decrease greatly after point 1 because the car body shape are streamlined. The pressure coefficient is very low at point 4 which located at top of windscreen. The pressure coefficient in roof gives negative value means very low total pressure due to the decrease in pressure drag. The pressure coefficient at the trunk increase because increase in flow velocity.

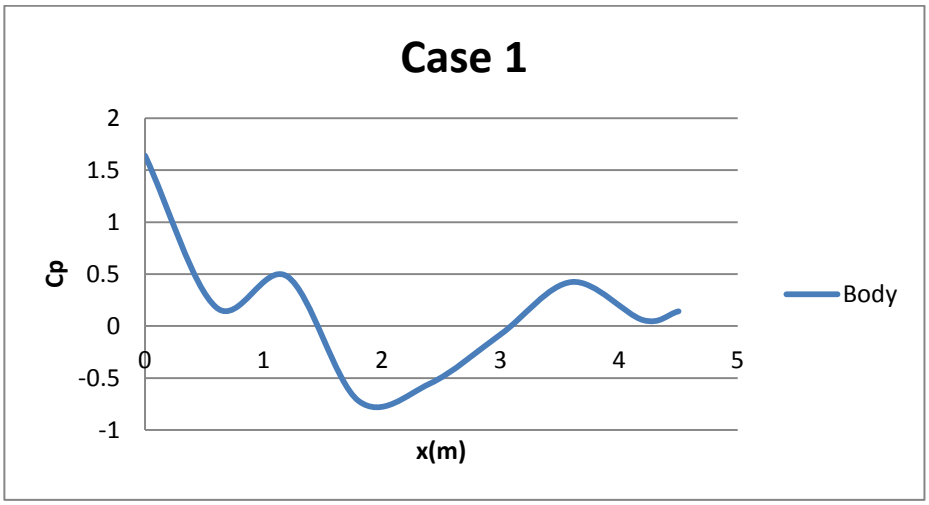

Figure 4.2: Pressure coefficient for case 1(without rear spoiler).

Table 4.2(a) is the result of total pressure and pressure coefficient obtained for case 2. Distance x in meter is the location of point along x-axis. Table 4.2(b) is the result for total pressure and pressure coefficient around spoiler for case 2. Four points has been located in different location along x-axis.

Table 4.2(a): Total pressure and pressure coefficient of car body for case 2.

No. of Points	X(m)	Total Pressure [kPa]	Pressure coefficient, C_D
1	0	102.3221	1.6884
2	0.6	101.5807	0.3653
3	1.2	101.5521	0.3142
4	1.8	100.9805	-0.7058
5	2.4	101.0970	-0.4979
6	3.0	101.1285	-0.4417
7	3.6	101.5096	0.2383
8	4.2	101.5405	0.2936
9	4.5	101.4801	0.1865

Table 4.2(b): Total pressure and pressure coefficient around spoiler for case 2.

X(m)	Total Pressure [kPa]	Pressure coefficient, C_D
4.05	101.5998	0.3995
4.28	101.5857	0.3743
4.20	101.6858	0.5529
4.50	101.5877	0.3779

Figure 4.3 is result of pressure coefficient distribution on top body of car and around the spoiler. The highest pressure coefficient value obtained at point 1 which is at front bumper due to stagnation point effect. The lowest pressure coefficient value at roof of the car which gives negative value. The pressure coefficient value is increase at the trunk of car gives positive value. The pressure coefficient value at the trunk of car for case 2 is higher than case 1 significantly shows the effect of the rear spoiler. The single-wing type spoiler was used for case 2. The pressure coefficient at the top of spoiler is higher than the pressure coefficient at top of car body. This is because the addition of spoiler disturbing the air flow around the car body cause increase in drag pressure.

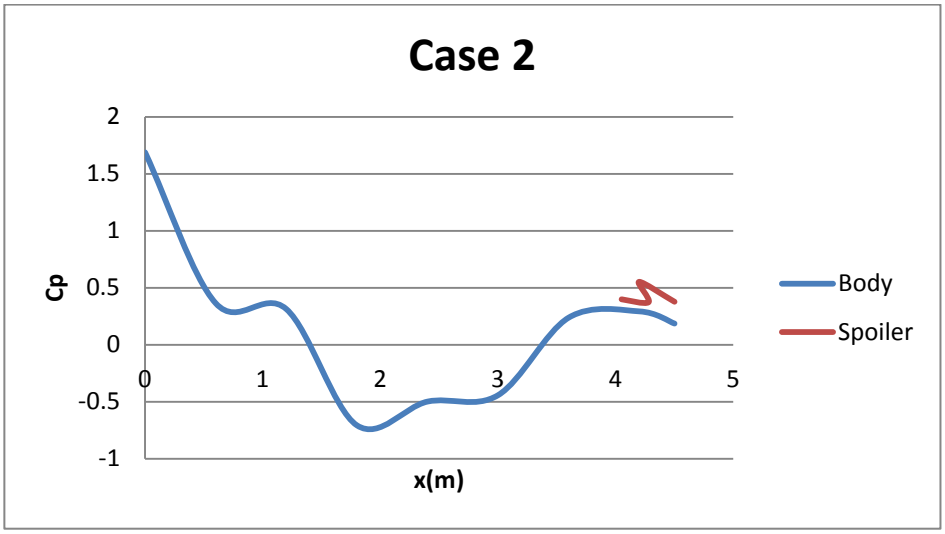

Figure 4.3: Pressure coefficient for case 2.

Table 4.3(a) is the result for case 3.Distance; x in meter is the location of point along x-axis. Table 4.3(b) is the result for total pressure and pressure coefficient around spoiler for case 3. Four points has been located in different location along x-axis.

Table 4.3(a): Total pressure and pressure coefficient of car body for case 3.

No. of Points	X(m)	Total Pressure [kPa]	Pressure coefficient, C_D
1	0	102.3232	1.6903
2	0.6	101.4512	0.1346
3	1.2	101.7360	0.6424
4	1.8	100.9733	-0.7187
5	2.4	101.0700	-0.5105
6	3.0	101.4924	0.2078
7	3.6	101.6456	0.4811
8	4.2	101.5950	0.3909
9	4.5	101.6247	0.5693

Table 4.3(b): Total pressure and pressure coefficient around spoiler for case 3.

X(m)	Total Pressure [kPa]	Pressure coefficient, C_D
4.05	101.7474	0.6627
4.28	101.5874	0.3772
4.20	101.6852	0.5518
4.50	101.6983	0.5752

The highest pressure coefficient value is at point 1 as shown in Figure 4.4 due to the pressure separation region. The pressure coefficient value decrease until point 2 caused by the streamlined body type. The pressure coefficient value increase at point 3 which located at windscreen due to the pressure drag. The pressure coefficient value on trunk always low(negative) as previous case. There is increase in pressure coefficient value at trunk of the car due to the addition of single-wing (with side cover) spoiler type.

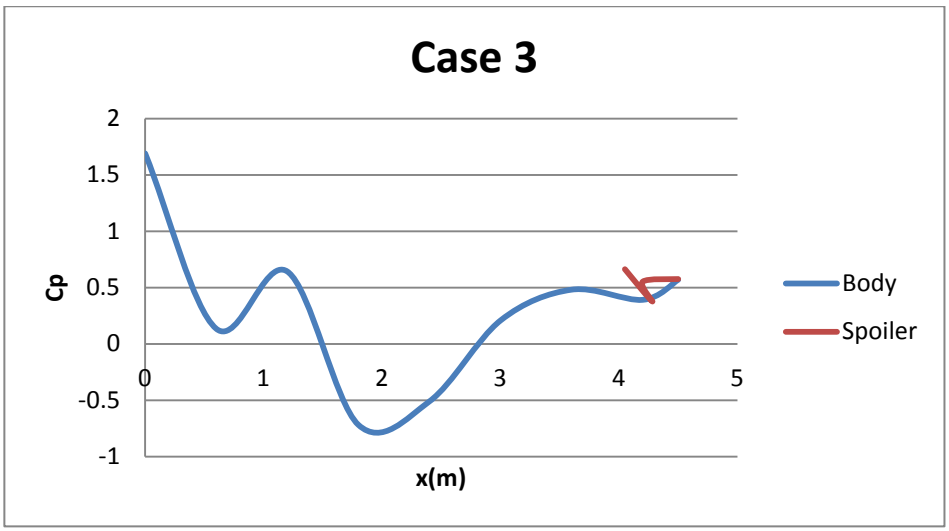

Figure 4.4: Pressure coefficient for case 3.

Table 4.4(a) is the result for case 4. Distance; x in meter is the location of point along x-axis. Table 4.4(b) is the result for total pressure and pressure coefficient around spoiler for case 4. Seven points has been located in different place along x-axis. More point located around spoiler so that the pressure distribution clearly can be notified.

Table 4.4(a): Total pressure and pressure coefficient of car body for case 4.

No. of Points	X(m)	Total Pressure [kPa]	Pressure coefficient, C_D
1	0	102.2774	1.6086
2	0.6	101.4984	0.2185
3	1.2	101.6296	0.4526
4	1.8	101.2618	-0.2039
5	2.4	100.8762	-0.8920
6	3.0	101.0503	-0.5812
7	3.6	101.9374	1.0019
8	4.2	101.7755	0.7129
9	4.5	101.6270	0.4470

Table 4.4(b): Total pressure and pressure coefficient around spoiler for case 4.

X(m)	Total Pressure [kPa]	Pressure coefficient, C_D
4.05	101.5377	0.2886
4.20	101.6729	0.5298
4.30	101.8486	0.8435
4.20	101.5129	0.2443
4.35	101.8505	0.8468
4.43	101.8905	0.9183
4.50	101.7878	0.7350

Figure 4.5 is pressure coefficient distribution for car body and rear spoiler for case 4. The highest pressure coefficient valued gained at point 1 which located at front bumper. The lowest pressure coefficient value gained at point 4 which located at roof of the car. Double-wing (upper wing behind lower wing) type spoiler used for case 4. This type spoiler gives highest pressure coefficient value at trunk portion compared to other type of spoiler. This is due to the design of the spoiler itself which disturbing air flow in wake region cause the pressure drag to increase. The upper wing which located at high stream flow experience greater pressure than the lower wing. This justified by Figure 4.5 where the pressure coefficient value at top wing is more than 1. The higher pressure gain at rear spoiler result in higher pressure at rear portion of the car trunk.

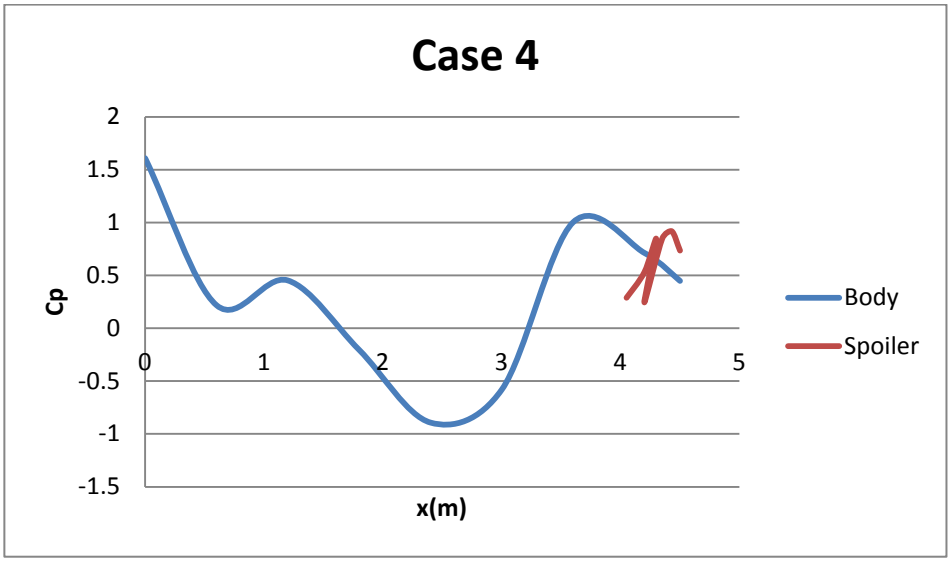

Figure 4.5: Pressure coefficient for case 4.

Table 4.5(a) is the result for case 5.Distance; x in meter is the location of point along x-axis. Table 4.5(b) is the result for total pressure and pressure coefficient around spoiler for case 5. Eight points has been located in different place along x-axis.

Table 4.5(a): Total pressure and pressure coefficient of car body for case 5.

No. of Points	X(m)	Total Pressure [kPa]	Pressure coefficient, C_D
1	0	102.3034	1.6551
2	0.6	101.6411	0.4731
3	1.2	101.5930	0.3872
4	1.8	101.2552	-0.2157
5	2.4	101.3039	-0.1286
6	3.0	101.6830	0.5479
7	3.6	101.5152	0.2484
8	4.2	101.4563	0.1427
9	4.5	101.3807	0.0083

Table 4.5(b): Total pressure and pressure coefficient around spoiler for case 5.

X(m)	Total Pressure [kPa]	Pressure coefficient, C_D
4.05	101.6191	0.4338
4.28	101.4342	0.1039
4.28	101.7405	0.6504
4.2	101.8003	0.7567
4.2	101.6543	0.4967
4.28	101.5439	0.2837
4.35	101.6154	0.4273
4.5	101.6291	0.4517

According Figure 4.6, the highest pressure coefficient obtained at point 1 where the pressure separation occurs due to the blunt body type. The pressure coefficient value decrease until point 4(lowest) which is located at roof of the car. The type of rear spoiler used in this case is double-wing (upper wing and lower wing aligned) type. The lower wing experience low pressure drag than the upper wing.

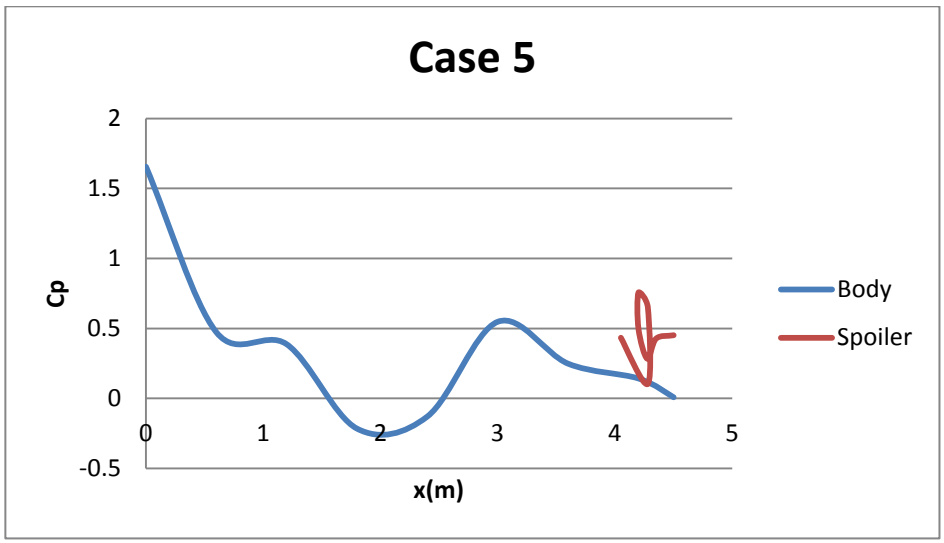

Figure 4.6: Pressure coefficient for case 5.

Table 4.6(a) is the result for case 6.Distance; x in meter is the location of point along x-axis. Table 4.6(b) is the result for total pressure and pressure coefficient around spoiler for case 6. Eight points has been located in different place along x-axis.

Table 4.6(a): Total pressure and pressure coefficient of car body for case 6.

No. of Points	X(m)	Total Pressure [kPa]	Pressure coefficient, C_D
1	0	102.3367	1.7144
2	0.6	101.6795	0.5416
3	1.2	101.8991	0.9335
4	1.8	101.1156	-0.4647
5	2.4	101.5267	0.2689
6	3.0	101.4851	0.1946
7	3.6	1016312	0.4555
8	4.2	101.6534	0.4950
9	4.5	101.6153	0.4271

Table 4.6(b): Total pressure and pressure coefficient around spoiler for case 6.

X(m)	Total Pressure [kPa]	Pressure coefficient, C_D
4.05	101.6534	0.4950
4.28	101.6393	0.4699
4.28	101.7106	0.5971
4.2	101.8557	0.8026
4.28	101.8170	0.8026
4.43	101.9379	0.7708
4.5	101.7243	0.6217
4.65	101.6409	0.4727

Figure 4.7 shows pressure coefficient for the car body and spoiler type of double-wing (upper wing in front of lower wing). The highest pressure coefficient value is at front bumper of the car while the lowest is at roof of the car. In this case, the upper wing located in front of bottom wing cause it experience less pressure as shown in Figure above. This due to the slope between rear window and trunk cause less air flow in that region (wake). These phenomena affect the effectiveness of rear spoiler which installed closed to the wake region.

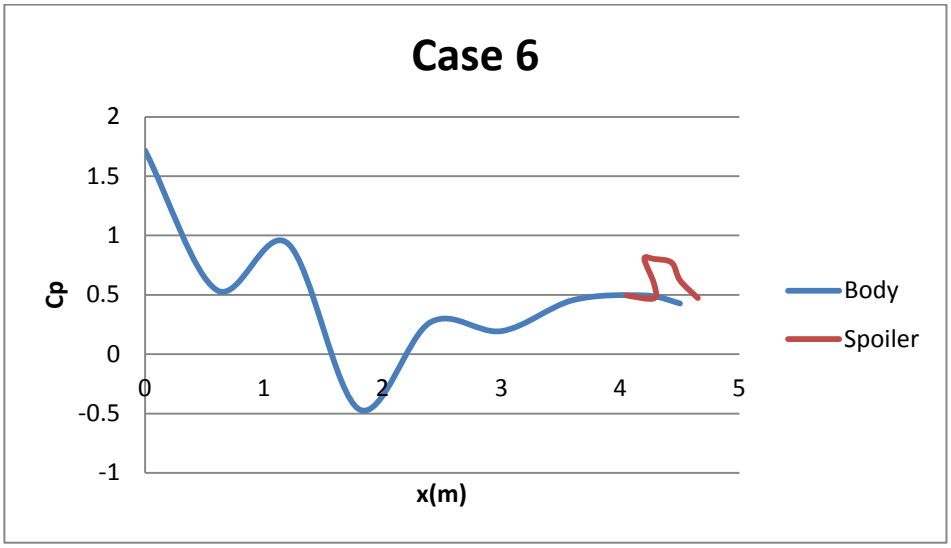

Figure 4.7: Pressure coefficient for case 6.

4.2.2 Drag and Lift Force

Force that acting along x-axis is drag force while force acting in z-axis is lift force. Table 4.7 is the result for drag force and lift force for all six model investigated.

Table 4.7: Drag force and lift force for six mode considered.

Case	Drag Force, F_D [N]	Lift Force, F_L [N]
Case 1	240.7144	225.8873
Case 2	242.0809	122.1820
Case 3	248.2078	157.4436
Case 4	267.2554	44.8811
Case 5	257.5524	64.6780
Case 6	246.4762	94.0268

Figure 4.8 is the lift force and drag force comparison between all six cases. It's clearly shown that adding of spoiler increase drag force and reduces lift force. The case 1 which is base model has lowest value of drag force and highest lift force which is 240.7144 N and 225.8873 N respectively. The maximum value of drag force is 267.2554N obtained by car model of case 4 while minimum value for lift force is 44.881 N obtained by car model case 4.

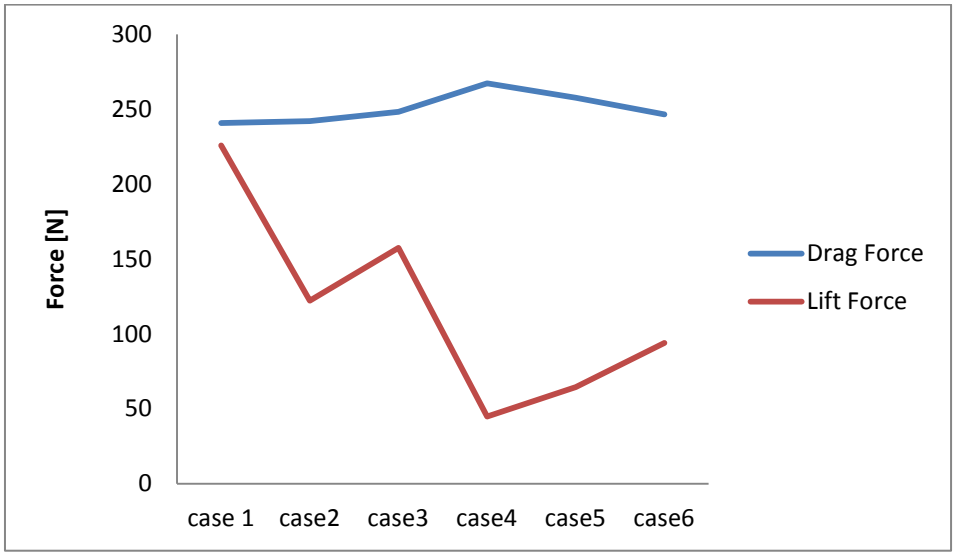

Figure 4.8: Comparison of drag force and lift force for six model considered.

The result from Table 4.7 used to calculate drag coefficient. Drag coefficient calculated using equation 2.5. The samples of calculation are as follow.

Drag Coefficient, C_D:

Drag Force, C_D = 240.714 N
Density, ρ = 1.225 kg/m³
Dynamic viscosity, μ = 1.862×10^{-5} kg/ms
Velocity, V = 30.56 m/s.
Frontal area, A = 1.98 m^2

Solution:

$$C_D = \frac{240.714\ \text{N}}{\frac{1}{2} \times \left(1.225 \frac{\text{kg}}{\text{m}^3}\right) \times \left(30.56 \frac{\text{m}}{\text{s}}\right)^2 \times (1.98\ \text{m}^2)}$$

$$= 0.2170$$

Table 4.8 shows drag coefficient for all cases considered.

Table 4.8: Drag Coefficient.

Case	Drag Force, F_D [N]	Drag coefficient, C_D
Case 1	240.7144	0.2170
Case 2	242.0809	0.2182
Case 3	248.2078	0.2237
Case 4	267.2554	0.2409
Case 5	257.5524	0.2321
Case 6	246.4762	0.2222

Figure 4.9 is comparison of drag coefficient of car model without rear spoiler (case 1) and car model with five different types of rear spoiler. Case 1 (without spoiler) gives lowest drag coefficient value. However the installation of rear spoiler increases the drag coefficient as shown in figure above. This is because the addition of rear spoiler increases the surface contact between the spoiler surface and the fluid flow. Thus its result in increase of drag force due to the friction of the air in the surface of the car. Case 4, case 5, and case 6 give higher value of drag coefficient than case 1 and case 2 is mainly because of double-wing type spoiler than been used in case 4, case 5, and case 6. The more extra part added, the more drag force produced. The highest value of drag coefficient produced by rear spoiler type of case 4 because of its design which alter the main flow of air that is major contributor of the drag force produced by the separation zone at the rear of car body.

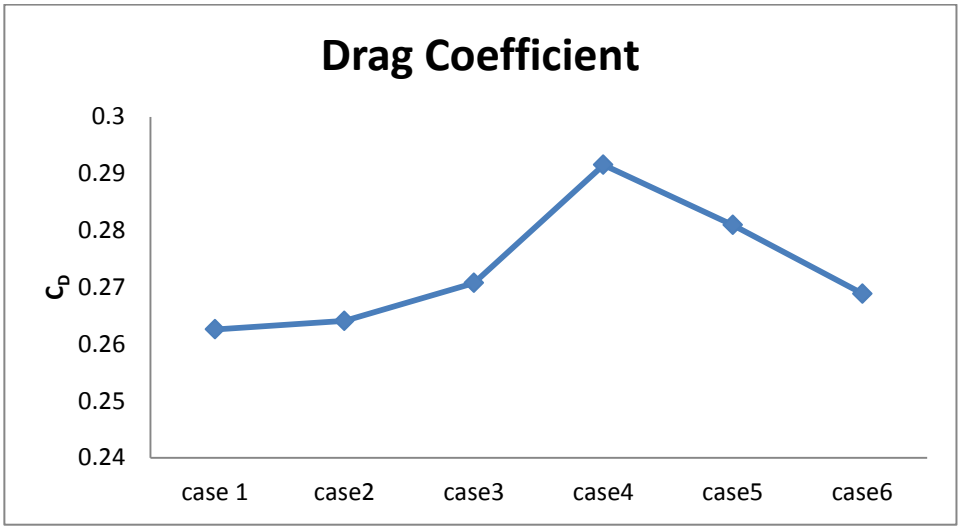

Figure 4.9: Comparison of drag force

The result from Table 4.7 used to calculate lift coefficient. Lift coefficient calculated using equation 2.2. The samples of calculation are as follow.

Lift Coefficient, C_L:

Drag Force, C_L = 225.887 N
Density, ρ = 1.225 kg/m³
Dynamic viscosity, μ = 1.862×10^{-5} kg/ms
Velocity, V = 30.56 m/s.
Frontal area, A = 1.98 m^2

$$C_L = \frac{225.887\ \text{N}}{\frac{1}{2} \times \left(1.225\ \frac{\text{kg}}{\text{m}^3}\right) \times \left(30.56\ \frac{\text{m}}{\text{s}}\right)^2 \times (1.98\text{m}^2)}$$

$$= 0.2036$$

Table 4.9 shows lift coefficient for all six cases considered.

Table 4.9: Lift coefficient.

Case	Lift Force, F_L [N]	Lift Coefficient, C_L
Case 1	225.8873	0.2036
Case 2	122.1820	0.1101
Case 3	157.4436	0.1419
Case 4	44.8811	0.0405
Case 5	64.6780	0.0583
Case 6	94.0268	0.0847

Figure 4.10 is comparison of drag coefficient between six cases. The lift force is generated due to the difference in pressure between the upper side and lower side of the car. Case 1 (without spoiler) gives highest lift coefficient value among other cases. The installation of rear spoiler effectively reduces lift force. The double-wing type spoiler produces lower lift force than single-type wing spoiler. Case 4, case 5, and case 6 is installed double-wing type spoiler while case 2 and case 3 is using single-wing type spoiler. Among these cases, there is greater pressure coefficient on the upper wing of the spoiler case 4 than other cases as shown in Figure 4.5. Therefore, its lift force is the minimum among all models.

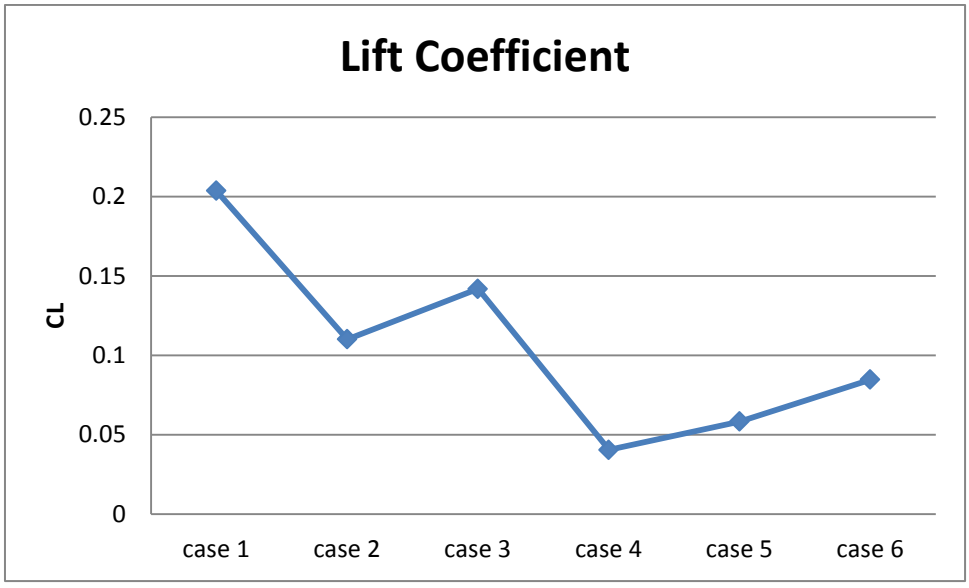

Figure 4.10: Comparison of Lift force.

4.3 Discussion

A symmetrical boundary condition was applied on the plane where the actual computational domain was split into two. On the plane upstream of the car, a constant velocity of 110 km/h which correspond to Re = 3.75×10^6 was applied. This speed used because 110 km/h is almost the maximum allowable highway speed limit in Malaysia. The plane downstream of the car model assumed a pressure outlet 1atm. Non-slip condition was applied on the entire solid surface. The Figure 4.2-4.7 shows the pressure distribution around the car. These figures also show the pressure distribution around the spoiler. Therefore the effect of different spoiler on the lift force can be estimated. For all the cases, the pressure coefficient in front of the bumper, wind screen and trunk were positive, but that associated to the roof was always negative. Figure 4.9 and Figure 4.10 shows the comparison of the drag force and lift force respectively for the six cases studied. When the spoiler installed on top of the trunk, the drag coefficient increases while lift coefficient decreases. The increases of drag force is due to the addition of extra part (spoiler) increasing the surface pressure. The decrease in lift force is caused by pressure increase in upper side of car which creates down force. For all the cases considered, the drag coefficient ranged from 0.2170(for case 1) to 0.2409(for case 4) whereas the lift coefficient varied from about 0.2036(for case 1) to approximately 0.0405(for case 4). This implies that among the design considered, the spoiler design case 4 produces the greatest vertical stability due to the minimum lift coefficient but without a spoiler yield the worst. The lift coefficient for all case was compares to the experiment findings by Tsai et al. (2007) and the comparison shows close similarity.

CHAPTER 5

CONCLUSION AND RECOMMENDATION

5.1 Conclusion

Lift force is the main issues for the road vehicles over the years. By reducing the lift force is the one of the solution to stability and handling particularly at high speed. It is well known that a large proportion of the lift is the result of pressure difference produced at the above rear end and under body of the vehicle and the understanding derived from the study of the wake structure is crucial in improving the road vehicle aerodynamic performance. For the road vehicles, it is basically three-dimensional bluff bodies in proximity to the ground.

By adding the aerodynamic devices like rear spoiler, the result will increase the pressure distribution at the rear trunk of the vehicles. From the result, it is shown an improvement by adding the rear spoiler as one of the aerodynamic devices. The design of spoiler in case 4 produces minimum lift coefficient which is 0.0405. The installation of spoiler type case 4 reduces lift coefficient from 0.2036 which is produce by case 1 (without spoiler) to 0.0405. This is due to the design type of spoiler in case 4 which cause greater pressure coefficient on upper wing of spoiler.

5.2 Recommendation

As for the future researches, the different length and different angle of attack of rear spoiler can be compared by simply attached to the same model to see the different of flow and also to determined is the design of the rear spoiler also influent the characteristic of the flow. Some other recommendation can be carried out:-

- Simulate the results with higher Re Number to minimize the lift coefficient.

- Increase refinement level (grid mesh size) of model to obtain more accurate result

- Further analysis on other parts on the model such as side mirror, side skirt, vortex generator, and others beside the well-known aerodynamic devices.

.

REFERENCES

Cengel, A.Y and Cimbala, M.J. 2006. *Fundamentals of Fluid Mechanics*. 1st ed. United State: Mc Graw Hill.

Choudhury, D. 1993. *Introduction to the Renormalization Group Method and Turbulence Modeling, Technical Memorandum TM 107*, Fluent Inc., Lebanon NH.

Ferlauto, M. and Marsilio, R. 2006. A Viscous Inverse Method for Aerodynamic Design. *Computer & Fluids*

Heisler, H. 2002. *Advanced Vehicle Technology*. Oxford: Elsevier Butterworth Heinemann.

Hirsch, C. 2007. *Numerical Computation of Internal and External Flows.* 2nd ed. Pages 1-20.

Ismail, J. 2008. Design and Analysis of Vortex Generator for a HEV. B.Eng. Thesis. University Malaysia Pahang. Malaysia.

Jeong, S.J., Kim, W.S. and Sung, S.J. 2007. Numerical Investigation On The Flow Characteristics and Aerodynamic Force of the Upper Airway of Patient with Obstructive Sleep Apnea Using CFD. *Journal of Medical Engineering & Physics.* **29.**

Katz, J. 1995. *Race Car aerodynamics*. Cambridge: Bentley Publication.

Kim, J.S., Kim, S., Sung, J., Kim, J.S. and Choi, J. 2006. Effect of an Air Spoiler on the Wake of the Road Vehicle by PIV Measurement. *Journal of Visualization.* **9**(4): 411-418.

Koike, M., Nagayoshi, T. and Hamamoto, N. 2004. Research on Aerodynamics Drag Reduction by Vortex Generators: 11-16

Najmudin, M. 2007. Analyze a New Spoiler for KUKTEM HEV. B.Eng. Thesis. University Malaysia Pahang. Malaysia.

Nor, M.B.M and Narayana, A. CFD Study of a Rear Spoiler Fitted to Sedan Car. Technical Report. University Technology Mara.

Paschkewit, J.S. (2006). A Computational Study of Tandem Dual Wheel Aerodynamics and the Effect of Fenders and Fairings on Spray Dispersion. Oxford University. Oxford.

Rajamani, G.K. 2006. CFD Analysis of Air Flow Interactions in Vehicle Platoons. B.Eng. Thesis. RMIT University. Australia.

Régert, T. and Lajos, Dr.T. 2006. The Effect of Wheels and Wheelhouses on the Aerodynamic Forces Acting on Passenger Cars. Technical Report. Budapest University of Technology and Economics. Hungary.

Tsai, C.H., Fu, L.M., Tai, C.H., Loung, Y., Huang. and Leong, J.C. 2007. Computational Aero-acoustic Analysis of a Passenger Car with a Rear Spoiler. *Journal of Applied Mathematical Modeling:* 3661-3673.

Watkins, S. and Oswald, G. 1999. The Flow Field of Automobile Add-ons-with Particular Reference to the Vibration of External Mirror. *Journal of Wind Engineering and Industrial Aerodynamics.* **83**.

.

APPENDIX A

GANTT CHART / PROJECT SCHEDULE FOR PSM 1

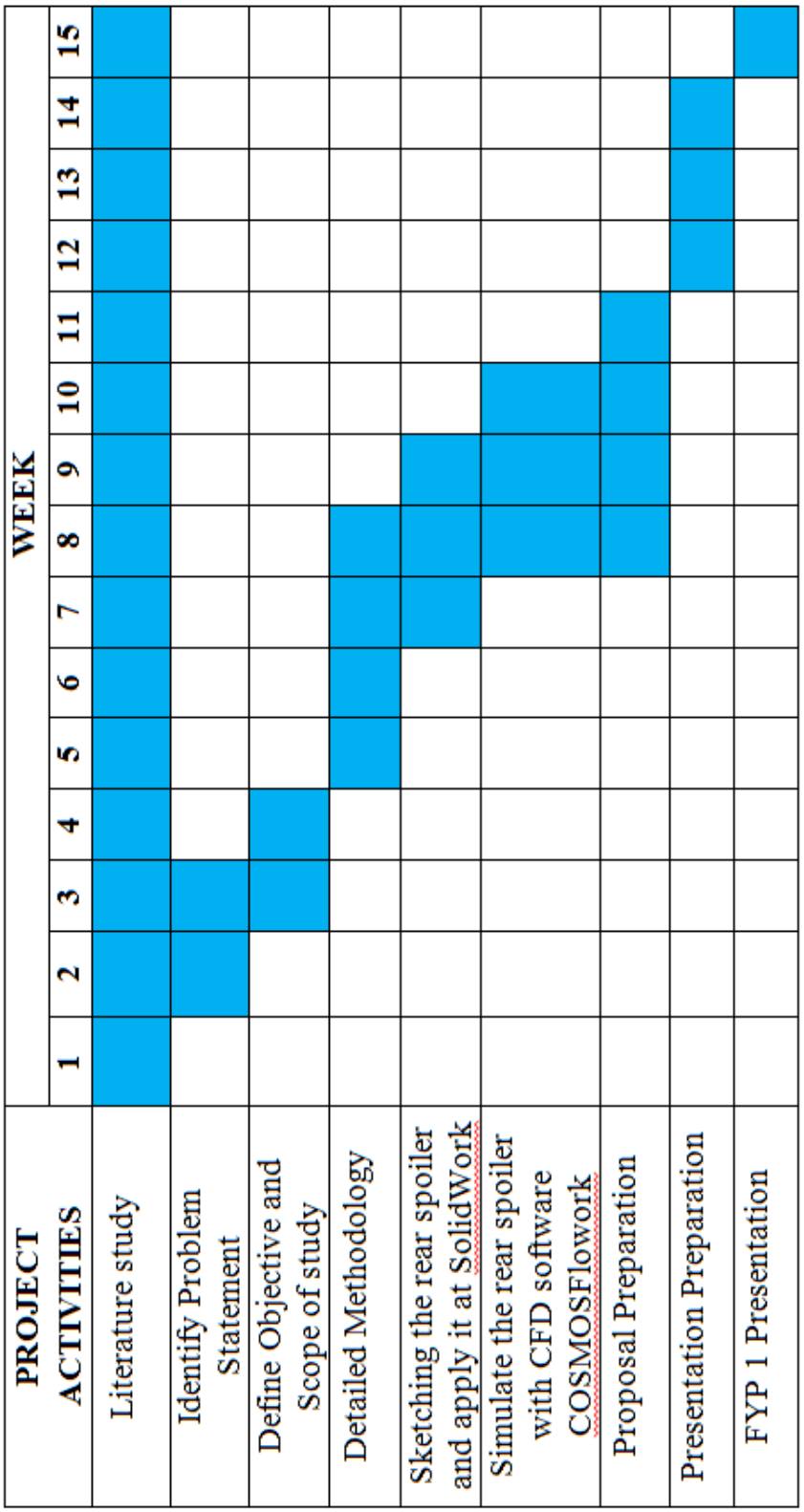

GANTT CHART / PROJECT SCHEDULE FOR PSM 2

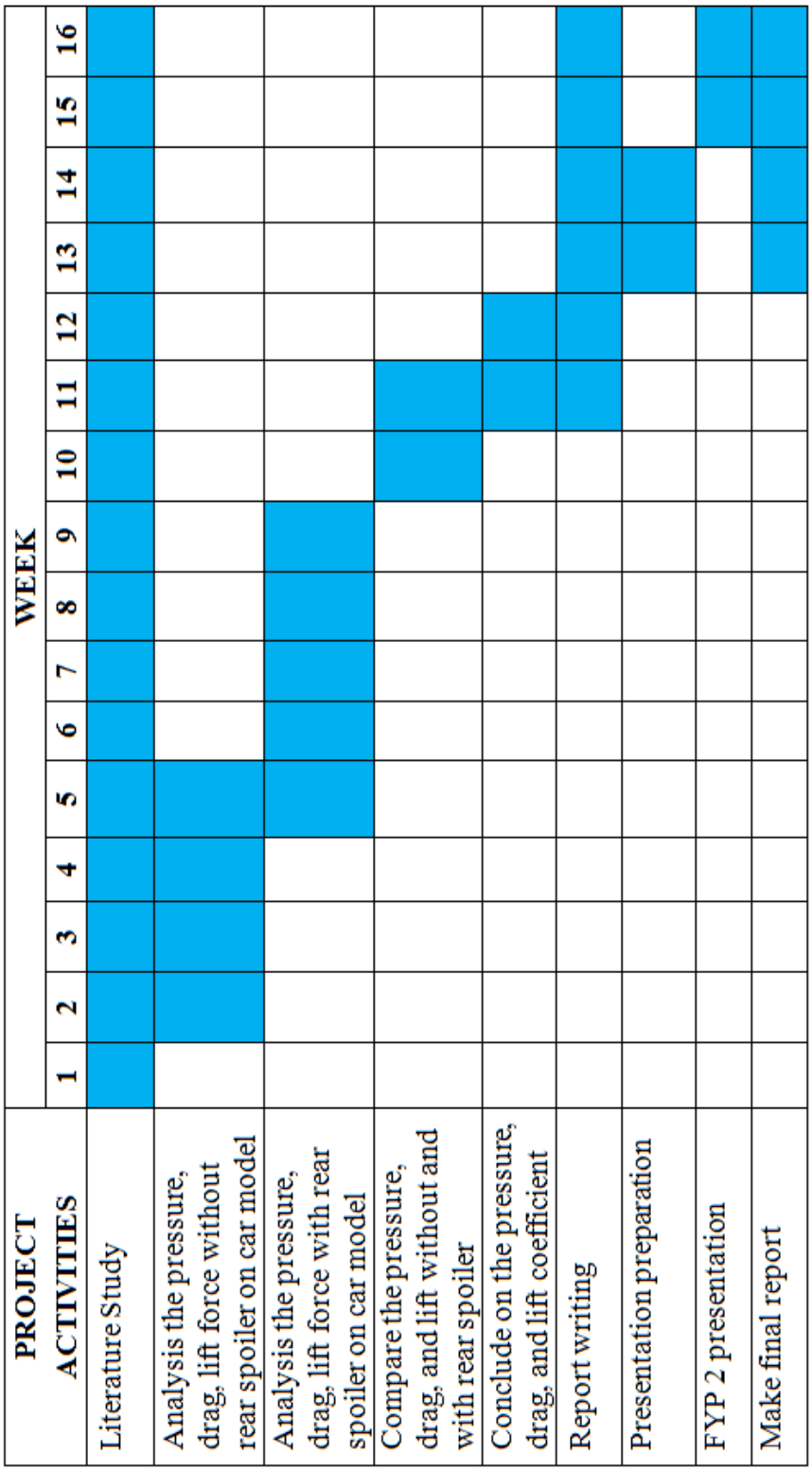

PROJECT ACTIVITIES	WEEK															
	1	2	3	4	5	6	7	8	9	10	11	12	13	14	15	16
Literature Study																
Analysis the pressure, drag, lift force without rear spoiler on car model																
Analysis the pressure, drag, lift force with rear spoiler on car model																
Compare the pressure, drag, and lift without and with rear spoiler																
Conclude on the pressure, drag, and lift coefficient																
Report writing																
Presentation preparation																
FYP 2 presentation																
Make final report																